
# Development of an LCMS-based assay for assessing the RISC loading of siRNA in-vitro

Master's thesis in Biotechnology

JONAS CARLSSON

DEPARTMENT OF CHEMISTRY AND CHEMICAL ENGINEERING

CHALMERS UNIVERSITY OF TECHNOLOGY
Gothenburg, Sweden 2024
www.chalmers.se

Master's thesis 2024

# Development of an LCMS-based assay for assessing the RISC loading of siRNA in-vitro

JONAS CARLSSON


CHALMERS
UNIVERSITY OF TECHNOLOGY

Department of Chemistry and Chemical Engineering
*Division of Chemistry and Biochemistry*
Chalmers University of Technology
Gothenburg, Sweden 2024

Development of an LCMS-based assay for assessing the RISC loading of siRNA in-vitro
JONAS CARLSSON



Supervisor: Mikko Hölttä, AstraZeneca
Examiner: Marcus Wilhelmsson, Department of Chemistry and Chemical Engineering

Master's Thesis 2024
Department of Chemistry and Chemical Engineering
Chemistry and Biochemistry
Chalmers University of Technology
SE-412 96 Gothenburg
Telephone +46 31 772 1000

Typeset in LaTeX
Printed by Chalmers Reproservice
Gothenburg, Sweden 2024

Development of an LCMS-based assay for assessing the RISC loading of siRNA in-vitro

JONAS CARLSSON
Department of Chemistry and Chemical Engineering
Chalmers University of Technology

# Abstract

Short interfering RNAs (siRNAs) have emerged as a potent new modality to target diseases previously considered undruggable. siRNAs utilize the endogenous RNA interference (RNAi) mechanism, wherein upon cellular entry, the siRNA forms a complex with the protein Argonaute 2 (Ago2), leading to the degradation of target mRNAs in a sequence-specific manner. This complex, known as the RNA-induced silencing complex (RISC), is formed through a process called RISC loading. Despite extensive research on the therapeutic potential of siRNAs, the intracellular dynamics of siRNA remain poorly understood, particularly the proportion of delivered siRNA that is loaded into RISC. Previous efforts to quantify RISC-loaded siRNA have not employed liquid chromatography-mass spectrometry (LC-MS) for this purpose. This study presents the development of an in vitro assay to determine the RISC loading of siRNA. By incubating an siRNA duplex in homogenized tissue, RISC formation is achieved in vitro. The RISC complex is then extracted using immunoprecipitation and digested using trypsin/lys-C. Ago2 and the complexed siRNA are the quantified in parallell via LC-MS. During the development the extraction conditions were optimized by studying several anti-Ago2 antibodies. It is also demonstrated that RISC is correctly formed during the incubation. This assay provides a novel approach for quantifying RISC-loaded siRNA, should serve as a tool to advance our understanding of siRNA dynamics within cells.

Keywords: LCMS, siRNA, RISC Loadin, immunoprecipitation.

# Acknowledgements

This project has been performed at and using the resources of AstraZeneca. I would like to extend my sincerest gratitude to the several people at the company that have assisted along the course of the project and have freely shared their knowledge and wisdom. A special thank you goes out to my supervisor for his endless patience.
I would also thank my family and friends for their support over the years. They made my eduation possible.

Jonas Carlsson, Gothenburg, June 2024

# List of Acronyms

Below is the list of acronyms that have been used throughout this thesis listed in alphabetical order:

| | |
|---|---|
| IP | Immunoprecipitation |
| LCMS | Liquid Chromatography coupled to Mass Spectrometry |
| m/z | Mass-to-Charge ratio |
| RISC | RNA Induced Silencing Complex |
| SRM | Selected Reaction Monitoring |
| siRNA | Short Interfering RNA |

# Contents

# 1
# Introduction

## 1.1 RNA Therapeutics and the RNA Induced Silencing Complex

The field of oligonucleotide therapeutics had its start in 1978 when single stranded antisense oligonucleotides were found to inhibit the replication of the Rous sarcoma virus (Zamecnik & Stephenson, 1978). Twenty years later, in 1998, the first ASO drug was approved when fomivirsen entered the market (Roehr B, 1998). In the same year it was discovered that transfecting Caenorhabditis elegans with double-stranded RNAs could interfere with the expression of specific genes in an apparently catalytic manner (Fire et al, 2006). This phenomenon was named RNA interference (RNAi), and the first drug that utilized the approach was approved in 2018 with patisiran (Adams et al., 2018; Kim, 2022).

The basis for RNAi are small double-stranded RNA strands. In the case of small interfering RNAs (siRNAs), this is a 21-25 nucleotide long duplex of two strands known as the ”guide” strand and the “passenger” strand. Upon entering the cytosol, the duplex is bound to a protein of the argonaute (Ago) family, and the guide strand is retained while the passenger strands is degraded (Pratt & MacRae 2009). The resulting complex is known as the RNA Induced Silencing Complex (RISC ), the formation of the complex is known as RISC loading and the siRNA is said to be loaded into the RISC (Iwakawa & Tomari, 2022).

After loading, the guide strand can go on to guide RISC to mRNAs whose sequences are complementary, "antisense", to its own. What happens next depends on what Ago protein the RISC contains, but out of all the Ago proteins, of which there are four in vertebrates, it is only Ago2 that has the ability to directly degrade mRNA. It is through this mechanism that RNAi is used to induce knock-down of specific genes (Pratt & MacRae, 2009; Iwakawa & Tomari, 2022). While the other members of the protein family also can affect gene expression by, for example, inhibiting protein translation, it is believed that Ago2 is the primary driver of the knock-down induced by siRNAs (Liu et al. 2004).

To improve its cellular uptake and to allow specific organs and tissues to be targeted an siRNA is often complemented with a delivery system. The siRNA can be enclosed in nanoparticles, commonly composed of various lipids, or conjugated to a ligand that binds to receptors on the surface of the target tissue (Biscans et al., 2018; Paunovska et al., 2022). Perhaps the most common means of delivery is by conjugating the siRNA with N-acetylgalactosamine (GalNac) (Springer et al., 2018). This molecule acts as a ligand to the asialoglycoprotein receptor which is

highly expressed and recycled with a high turnover in liver tissue (Nari et al., 2014). As this means that siRNA can easily and reliably be delivered to the liver, several projects have explored using GalNac conjugated siRNA to target and treat diseases in the liver (Butler et al., 2016; German & Shapiro, 2019; Springer et al., 2018)
Once delivered to a tissue the siRNA is taken up by the cells via endocytosis and encased in a vesicle, an endosome. To form RISC, it is necessary for the siRNA to first escape from this endosome. By what mechanism and what fraction of the siRNA concentration that proceeds to escape is yet not fully understood, but a commonly cited value is that around 1% of the confined siRNA escapes (Dowdy 2023; Gilleron et al. 2023; Vocelle et al. 2020)
While siRNAs have a large potential to treat diseases that more conventional drugs cannot access and have been shown to be highly efficient with long *in vivo* half-lives and potent knock-down at low dosages, there is still much that remains unknown about how they behave upon entering the cell (Kim, 2022).
While the total amount of siRNA can be measured in vivo using the methods described below, this value does not correlate well with the resulting knock-down as it fails to take into account factors such as endosomal escape and RISC loading (Abrams et al., 2010; Mesalchin et al., 2007). It is therefore suggested that measuring the amount of RISC loaded siRNA would provide a better correlation with knock-down, and further would allow researchers to characterise delivery vehicles and chemical modifications in greater detail (Hu et al., 2020). Previous publications have described methods to do this by extracting RISC with immunoprecipitation using antibodies specific to Ago2, or by using oligo probes coupled to magnetic beads. The dominant method of quantifying the extracted siRNA has been qPCR (Flores-Jasso et al., 2013; Pei et al., 2010; Zhang et al., 2010; Zheng et al., 2013)

## 1.2 Bioanalysis

### 1.2.1 Oligonucleotides

Bioanalysis, being the quantitative measurement of a compound in a biological matrix, is an important tool in drug development as it can be used to study the pharmacokinetic and pharmacodynamic properties of candidate drugs (Pandey et al., 2010; Thakur et al., 2021). The process can be divided into two steps. The first is sample preparation, where an analyte is separated from contaminating components of the sample matrix that can interfere with the later analysis (Clark et al., 2016). The second step is the analysis itself, where the analyte is quantified (Pandey et al., 2010). Here methods applicable to oligos and protein will be discussed. For the extraction of oligos, several alternatives exist. One of the most common strategies is liquid-liquid extraction (LLE) where cell lysates are mixed with an organic solvent. As the mixture separates into an aqueous and an organic layer, the charged oligos will remain in the aqueous layer while non-polar contaminants, such as denatured proteins and lipids, will be dissolved in the organic one (Clark et al., 2016; Nuckowski et al., 2018). An alternative is solid phase extraction (SPE) where the sample is introduced to a solid material that retains the oligo. Contaminants that are also retained can be washed away separately from the oligo using wash buffers

of various compositions, after which the oligo can be eluted by washing with, for example, 50% acetonitrile (Clark et al., 2016; Nuckowski et al., 2018). Several options also exist for the analysis and quantification of oligos after extraction. These include hybridization assays, quantitative PCR (qPCR) and liquid chromatography coupled with mass spectrometry (LC-MS) (Tremblay & Oldfield, 2009). As the name implies, these assays utilize the ability of single stranded oligos to hybridize with complementary sequences. A probe with sequence complementary to that of the oligo being analyzed is fixed to the bottom of a well in which the sample is incubated and upon encountering the probe the oligo will bind to it via base pairing. The probe can be a fluorescent molecule, and by degrading and washing away any single-stranded, unhybridized probes that remain after incubation it is possible to quantify how much of the desired oligo is present in a given sample by measuring the remaining fluorescence (Deshpande et al. 2016).

qPCR is a variation on the PCR protocol which in addition to the oligo primers used for amplification of specific sequences also includes fluorescent probes. These probes are coupled to both a fluorophore and a quencher, and if a probe is hybridized with an oligo when amplification starts it will be cleaved. This separates the fluorophore and the quencher which generates a fluorescent signal proportional to the number of copies of the oligo that was amplified. By measuring this signal one can quantify how many copies of an oligo is present in a sample (Arya et al., 2005). Finally, LC-MS works by separating the separating the compounds in a sample with chromatography with the final analysis being performed with mass spectrometry. A common type of chromatography in bioanalysis is reverse phase LC where the sample is introduced onto a column containing a non-polar stationary phase, commonly C18, and eluted using a polar mobile phase, commonly water. Compounds that are non-polar will interact more strongly with the stationary phase via electrostatic interactions and will be retained for longer than polar compounds, which is how separation is achieved. This works well for proteins and peptides as they frequently contain hydrophobic structures that allow them to interact well with the column (van de Merbel, 2019). However, reverse phase is less well suited for the analysis of oligos due to their negatively charged phosphate backbone. This renders them highly polar and which in turn means that they will only interact weakly with the column, and more suitable options include hydrophilic interaction chromatography and ion pair chromatography. The former uses polar stationary phases to ensure retention of hydrophilic compounds while the latter uses the same, hydrophobic stationary phase as reverse phase LC but adds an ion pair reagent to the mobile phase. The reagent binds to the phosphate groups in the backbone of the oligo to neutralize their charges and presents a more hydrophobic surface to the column to increase retention (Liu et al. 2022;).

Detection then achieved by coupling the LC system to an MS system. The MS characterises what compounds elute from the LC system by ionising them and measuring the resulting mass to charge ratio (m/z). One of the most common means of ionization in bioanalysis is electrospray ionization where the liquid eluting from the LC is nebulized by spraying it through a capillary. By then applying high heat and an inert gas in the presence of a high voltage, the droplets will gradually evaporate until they reach a critical size where the ions in the liquid will repel each other and

disperse into the gas phase (Ho et al., 2003; Korfmacher, 2005). The ions will then enter the MS where an electrical field is applied which alters their path of travel based on the mass-to-charge ratio (m/z) of the ions. This is used to select for specific m/z values by ensuring that ions that do not match said values will strike the wall of the MS. Ions that do match will instead reach the detector and generate a signal (Ho et al., 2003).
The exact details of this process may vary depending on the goal of the analysis. To achieve a high degree of specificity one can use selected reaction monitoring (SRM) on triple quadrupole (TQ) instruments. In a TQ-MS three quadrupoles are placed in series and used to provide two stages of filtering. The ionised compounds enter the first quadrupole (Q1) which filters away all ion that are not of a specific m/z, ions that do have the specified m/z value are known as ”parent ions”. The parent ions are then fragmented in the second quadrupole (Q2), also known as a collision cell. The third quadrupole (Q3) selects for a ”daughter ion” by filtering away all fragments that don't carry a specific m/z value. The daughter ions can then go on to be detected and generate a signal. The results can be read as a chromatogram where the intensity of the signal is plotted against the elution time (Ebhardt, 2013). A pairing of a parent and daughter ion is known as a “transition” (Ebhardt, 2013).

### 1.2.2 Proteins

For the bioanalysis of proteins the process is similar, but with several differences. While it is possible to use SPE and LLE for the extraction proteins, a more common option is to utilize antibodies to capture specific proteins (van der Merbel, 2019; Wilffert et al., 2015). One technique in this family is immunoprecipitation, where an antibody that is specific to the protein of interest is immobilised to a solid support, commonly magnetic beads, before being added to a sample. By then magnetically separating the beads from the sample liquid the protein of interest can in turn be separated from any contaminants that were not captured by the beads (van der Merbel, 2019; DeCaprio & Kohl, 2020).
While LCMS is a suitable alternative for the quantification of proteins, the process is more complex than for oligos. While it is possible to quantify the intact protein, the size of the protein will lead to a range of m/z values being generated (Bults et al., 2019; Tassi et al., 2018). As this complicates the analysis, proteins can instead be broken down into peptides which are more easily ionizable in the MS. This is commonly achieved by digesting the protein enzymatically using trypsin which cuts after the C-terminal of the amino acids lysine and arginine. This means that the same peptides will be generated consistently, making quantification more reliable than if peptides were generated at random. A peptide that is quantified in place of the whole protein is known as a “surrogate peptide” (Cheng et al., 2014; van de Merbel et al., 2019).
Surrogate peptides should fulfil certain criteria to allow for consistent quantification. They should be of suitable length for analysis in LC-MS, which in practice this is around six to twenty amino acids. They should also not contain amino acids, such as methionine and tryptophan which can oxidise. If the sequence from which the peptide is generated contains long, continuous or alternating sequences of lysine

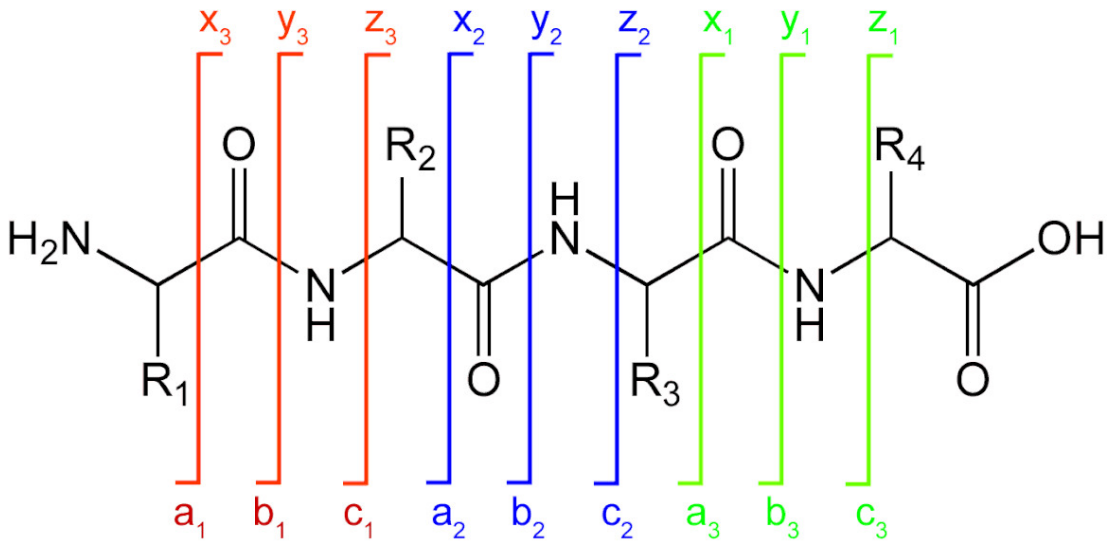


**Figure 1.1:** Nomenclature for peptide fragmentation. Shared under GNU Free Documentation License and CC BY-SA 3.0 DEED. Original author is Kkmurray.

and arginine the digestion by be interfered with and as such they should be avoided as well (Cheng et al., 2014). The fragments generated by a peptide are named according to their structure (Figure 1.1). Fragments that contain the C-terminus of the peptide are named x, y or z ions depending on where in the C-terminal amino acid fragmentation occurs, while fragments that contain the N-terminus are named a, b or c ion following the same logic.
Any final decisions on which peptides serve the best as surrogate should be made on experimental data. SRM based methods run on TQ-MS are not necessarily the best tools to use in the early stages of evaluating surrogate candidates, since these methods may not have the necessary resolution to separate peptides of similar mass that elute at the same time. To screen all the peptides that are generated by digestion, high resolution MS can be used instead. Using detectors with a very high resolution one can study all transitions generated by all peptides eluting at a given time. Time of flight or OrbiTrap detectors are usually used for this purpose (Li& Smith, 2021; Mann & Kelleher, 2008). Software tools exist to aid in all steps of this process. An example is the free and open source Skyline, which in addition to predicting what peptides will be generated in digestion can also analyse data generated via SRM and high resolution MS. It can also predict what instrument parameters are likely to be optimal for the given transitions (Cheng et al., 2014; Pino et al., 2017; Maclean et al. 2010).

### 1.2.3 Matrix effects

Even after extraction, matrix effects might remain an issue and affect the signal of the analyte. This might manifest in, for example, signal suppression where the signal of the analyte is lowered by the presence of a compound which elutes at the same time. One strategy to correct for this is to add an internal standard (IS) to every sample at a known concentration. By dividing the signal generated by the analyte

by the signal generated by the IS one can compensate for any variation induced by sample preparation or by the instrument itself. The choice of IS matters, and it should be chemically similar to the analyte and be ionized in a similar. For the quantification of surrogate peptides one can use a synthetic peptide with the same sequence that has been labelled with a stable isotope. (Jeanne Dit Foque et al., 2018; Panuwet et al. 2016). In the IS used in this article, all 12C atoms of an amino acid in a peptide with a 13C, generating a stable isotope labeled internal standard (SIL-IS) that should behave the same way as their counterparts generated through digestions in the LC and ionization as the surrogate, but due to the difference in mass it they can be separated in the MS.
To relate the signal generated by the analyte in the MS it is common practice to use standard curves where analyte is spiked into a matrix and subjected to the same extraction and analysis as the samples (Cheng et al., 2022; Moosavi & Ghassabian, 2018). Ideally the standard curve would be prepared in a blank matrix of the same composition as the samples, but if the analyte is endogenous this might not be possible. A solution this problem is the use of a surrogate matrix, which is an an alternate blank matrix, such as buffer or plasma, which is used instead of the sample matrix. A second solution is standard addition, where a curve is constructed in the sample matrix itself by spiking the analyte into the sample at varying concentrations. By performing linear regression, the native concentration in the sample can be read from the negative x-intercept of the generated curve (Moosavi & Ghassabian, 2018).

### 1.2.4 Goal of the project

To the author's knowledge, no publication has currently described quantifying both parts of RISC in a single assay, nor has any previous article used LC-MS to measure RISC loading. The purpose of this project was therefore to develop a quantitative assay using LC-MS to determine the molar ratio between RISC loaded siRNA and the total intracellular amount of Ago2.

# 2
# Materials and Methods

## 2.1 Extraction

### 2.1.1 Homogenisation

The tissue was mixed with ice cold lysis buffer at a ratio of 100 µl tissue to 900 µl lysis buffer in a reinforced plastic tube (Bertin Instruments, Catalog no. P000943-LYSK0-A)). Six to eight metal beads (Bertin Instruments, Catalog no. P000925-LYSK0-A) were then added before homogenization at 6500 RPM for 20 seconds, repeated three times and allowing the homogenate to cool down on ice for 30 seconds before each cycle. The homogenate was then centrifuged at 10,000 RCF and 4 °C for ten minutes before being used or aliquoted in protein LoBind tubes (Eppendorf, Catalog no. 022431018) and frozen at -80 °C. The lysis buffer used were 1% Tween-20 (Merck, P1379-25ML) in 50 mM Tris-HCl (ThermoFisher, Catalog no. 15567027), 1% NP40 (ThermoFisher, Catalog no. 85124) dissolved in 50 mM Tris-HCL, RIPA lysis buffer (ThermoFisher, Catalog no. 89900) and MSD lysis buffer (Meso Scale Discovery, Catalog no. R60TX-2)

### 2.1.2 Measurement of Total Protein Concentration

The total protein concentration of homogenised tissues was measured using a Pierce BCA Assay Kit (ThermoFisher, Catalog no. 23225) and was performed in a clear, flat Bottom 96 well plate (ThermoFisher, Catalog no. 442404). A standard curve was constructed by diluting the included BSA standard with MQ water according to the instructions of the manufacturer. Samples were diluted from ten times up to 100,000 with deionized water, diluting with a factor of ten at each step. 25 µl of each standard or sample was added to the wells in the plate, in duplicate. The plate was then mixed using a plate shaker for 30 seconds and left to incubate for 2 hours at room temperature. After incubation, the absorbance of each well at 562 nm was measured using a SpectraMax i3x plate reader (Molecular Devices). A standard curve was then generated in Excel using linear regression and used to calculate the total protein concentrations of the homogenates.

### 2.1.3 Preparation of Antibody-Bead Conjugate

A list of the antibodies used as well as their vendors can be seen in Table 1.
Antibodies that came in buffers containing primary amines were subjected to a buffer exchange as these would interfere with the biotinylation. The antibodies

| Clone name | Supplier | Catalog number | Reactivity |
|---|---|---|---|
| JF0992 | ThermoFisher | MA5-32520 | Mouse, Rat, Human |
| EPR10411 | Abcam | ab186733 | Mouse, Rat, Human |
| 11A9 | Merck | MABE253 | Human |
| 2E1C-1C9 | Novus Biologicals | H00027161-M01 | Mouse, Rat, Human, Pig, Primate, Xenopus |
| 2D4 | Wako/FujiFilm | 4987481480629 | Mouse |
| 4G8 | Wako/FujiFilm | 4987481480698 | Human |
| Monoclonal Rabbit IgG Clone 036 | SinoBiological | 50683-R036 | Mouse, Human |

**Table 2.1:** Clone names, supplier and reactivity as reported by the vendors of the antibodies that were screened.

were diluted to a total volume of 500 µl in PBS and then being concentrated down to 50 µl of liquid using centrifugal filters with a 30 kDa molecular weight cut off (Sigma Aldrich). The filter was then centrifuged at 14,000 x g for three minutes. This process was repeated four times. After the final concentration the filter was washed with 50 µl of PBS and the liquid was recovered by inverting the filter and centrifuging at 1500 x g for 1 minute. The final concentration of antibody in the liquid was measured using a NanoDrop spectrophotometer (ThermoFisher).
Following the instructions of the manufacturer one vial of biotin was diluted in 180 µl of MQ water. Biotin was then added to antibodies at a 1:20 molar ratio of biotin to antibody. The mixture was incubated at room temperature for 30 minutes before being desalted using desalting spin columns (ThermoFisher, Catalog no. 89882).
The columns were first centrifuged at 1500 x g for 1 minute to remove the storage solution. 100 µl of biotinylated antibody was then added to the column which was then centrifuged again at 1500 x g for 20 minutes. The eluted antibody was then aliquoted in Protein LoBind tubes (Eppendorf, Catalog no. 0030108094) and stored at -80 °C.
To conjugate the antibodies to the magnetic beads, 275 µl of Pierce Streptavidin Magnetic Beads (ThermoFisher, Catalog no. 12321D) were washed three times in 1 ml of 0.05% Tween-20 in PBS. The beads were separated from the liquid using a magnetic rack between each wash (ThermoFisher, Catalog no. 10723874) for 1 minute. The magnetic beads were then incubated with 1.7 µl of biotinylated antibody in 21.5 µl of PBS for 30 minutes at room temperature while mixed at 800 rpm. The mixture of antibody conjugated beads, the ”slurry”, was then washed three times with 0.05% Tween-20 in PBS before being resuspended in 137.5 µl of PBS.

### 2.1.4 Preparation of standard curves

Standard curves for the quantification of Ago2 were prepared via serial dilution of recombinant Ago2 according to the dilution series scheme in Table 2.2. All recombinant proteins as well as to which species their amino acid sequence belongs is listed in Table 2.3.
Diluents were 50 mM Tris-HCl and mouse blood plasma diluted 1:5 with either 50 mM Tris-HCl, MSD lysis buffer or RIPA lysis buffer. 50 µl of each standard was used as sample and subjected to immunoprecipitation.
Standard curves for the quantification of Ago2 were prepared via serial dilution of SOD1 duplex according to the dilution series scheme in Table 2.4. Diluent was

crashed plasma diluted with deionized water, prepared as described above.

| Stock (uL) | Diluent (uL) | Ago2 (ng/mL) |
|---|---|---|
| 10 | | 100000 |
| 10 | 990 | 1000 |
| 125 | 125 | 500 |
| 110 | 110 | 250 |
| 110 | 110 | 125 |
| 110 | 110 | 62,5 |
| 110 | 110 | 31,25 |
| 110 | 110 | 15,625 |
| 110 | 110 | 7,8125 |
| 0 | 100 | 0 |

**Table 2.2:** Scheme of serial dilution to prepare standard curves of recombinant Ago2

| Vendor | Catalog no. | Species | Mass (kDa) | Length (Amino Acids) |
|---|---|---|---|---|
| Active Motif | 31486 | Human | 104 | 859 |
| OriGene | TP328592 | Human | 93.4 | 856 |
| SinoBiological | 50683-M07B | Mouse | 99 | 860 |

**Table 2.3:** List of all recombinant proteins used in the project. The mass and length are as stated by the vendor, if available.

### 2.1.5 Immunoprecipitation

The immunoprecipitation was performed in a 96 well format in 0.5 ml protein LoBind plates (Eppendorf, Catalog no. 0030504100). 50 µl of sample was mixed with 200 µl of 50 mM Tris-HCl, pH 8.0, containing 0.1% BSA (Rossix) and 5.2 – 40 µl of slurry depending on the experimental conditions. Incubation was performed at 1000 rpm for 1 hour at room temperature.
In cases where samples were diluted to different dilution factors, the sample was diluted before immunoprecipitation with 50 mM Tris-HCl such that the final dilution in the plate would be correct. For example, if the final dilution was to be 25 times, the sample was diluted 5 times before immunoprecipitation was performed.
After incubation, the beads were washed twice with 450 µl of 0.05% Tween- 20 in PBS, once with PBS and a final time with 50 mM Tris before being resuspended in 50 µl of Tris. The samples were then digested by adding 10 µl of 50 µl/ml Trypsin/Lys-C (ThermoFisher, Catalog no. A41007 ) in 50 mM Tris-HCl (ThermoFisher) to each well and incubated overnight at 37 ° C while being shaken at 1000 rpm.

### 2.1.6 Sample work up

After digestion the plate was centrifuged at 2500 RCF and 4 °C for 10 minutes. Samples were then magnetically separated from the beads and 40 µl of liquid was

| Stock (uL) | Diluent (ul) | SOD1 (nM) |
|---|---|---|
| 20 | | 100000 |
| 10 | 990 | 1000 |
| 2.5 | 245 | 10.10101 |
| 110 | 220 | 3.367 |
| 110 | 220 | 1.12233 |
| 110 | 220 | 0.37411 |
| 110 | 220 | 0.1247 |
| 110 | 220 | 0.04157 |
| 110 | 220 | 0.01386 |
| 0 | 220 | 0 |

**Table 2.4:** Scheme of serial dilution to prepare standard curves of SOD1 siRNA.

transferred to a new plate. To ensure that no beads remained in the liquid, the procedure was repeated once more. The samples were then diluted with 40 µl of crashed plasma. The diluent was produced by crashing mouse plasma with methanol (Sigma-Aldrich, Catalog no. 1060351000) at a ratio of 1:2.3 plasma to methanol, centrifuging at 3000 RCF for 5 minutes and diluting the supernatant 8 times with deionized water.
40 µl of sample were then transferred to one of two 96 well PCR plates (ThermoFisher, Catalog no. AB0800L) containing 10 µl of deionized water with 3.5% formic acid (FA) and 2.38 pmol/ul of stable isotope labelled internal standard peptides (SIL-IS) (ThermoFisher) or 21 nM of MALAT1 IS, depending on if Ago2 or siRNA were to be quantified.
The C-terminal lysine or arginine of the peptides used as IS were modified by the vendor with an isotopic label. The sequences, what amino acid was changed and how this altered the mass of the peptide can be seen in Table 2.5.

| Sequence | Modification |
|---|---|
| VLQPPSILYGG[R] | Six $^{13}$C replacements |
| SGNIPAGTVDT[K] | Six $^{13}$C replacements |
| ELLIQFY[K] | Six $^{13}$C replacements |

**Table 2.5:** Show the sequences and modifications of peptides used as internal standards. Modified amino acids are indicated with brackets

## 2.2 Analysis

### 2.2.1 Selection of Surrogate Peptides

To select potential candidates for surrogate peptides, recombinant Ago2 (Active Motif) at a concentration of 0.1 µl/ul was digested with Trypsin/Lys-C overnight at 37 °C. The solution was then diluted 1:10 with deionized water containing 5% ACN and 0.1% FA. Analysis was performed using an OrbiTrap system (Exploris

480, ThermoFisher). The data was imported into Skyline and filtered by removing peptides containing the following: methionine, tryptophan, arginine-arginine, lysine-lysine or arginine-lysine sequences, and arginine or lysine followed by proline. From the remaining peptides, the transitions that generated the strongest signal were selected for further evaluation using triple quadrupole MS.
The mobile phases used, hereafter referred to as mobile phases A and B, were, respectively: A: MQ water mixed with 0.1% formic acid (FA)(ThermoFisher, Catalog no. PI28905) and 2% acetonitrile (ACN)(Thermofisher, catalog no. A955-500M; Merck, Catalog no. 1000291000), B: ACN. The gradient is shown in Table 2.6
Data collection was performed using data dependent acquisition. Full scan was performed at a resolution of 120,000 over a m/z range of 350-1200. Charge states of 2-5 were included. Fragmentation was triggered at an intensity threshold of 1000. Normalised collision energy of 30% was used. Scan range was defined based on a first m/z of 120. Data type was centroided. 10 scans were performed in total.

| **Time (min)** | **%A** | **%B** |
|---|---|---|
| 0 | 95 | 5 |
| 1.0 | 95 | 5 |
| 5.0 | 55 | 45 |
| 6.0 | 20 | 80 |
| 7.5 | 20 | 80 |
| 7.7 | 20 | 80 |
| 7.9 | 95 | 5 |

**Table 2.6:** Shows gradient used to separate tryptic Ago2 peptides before analysis with OrbiTrap MS

### 2.2.2 Liquid Chromatography - Mass Spectrometry

#### 2.2.2.1 Ago2

For the quantification of Ago2, the immunoprecipitated samples were analyzed using several different LC-MS systems. LC systems used were ACQUITY UPLC and ACQUITY Premier systems (Waters). MS systems used were TQ-S, TQ-XS and TQ Absolute (Waters). In all cases 5-10 µl of sample was injected onto a ACQUITY UPLC BEH 1.7 um, 2.1 x 50 mm C18 column (Waters, 186002350) at a temperature of 60 °C. Mobile phases A and B, were, respectively: A: MQ water mixed with 0.2% FA and 2% acetonitrile (ACN), B: ACN mixed with 2% FA. The gradient is shown in table 7. Flow rate was 0.5 ml/ml. Unless otherwise specified the transitions monitored can be seen in Table 8. Collision energies and cone voltages were predicted using Skyline (MacLean et al., 2010)

#### 2.2.2.2 siRNA

The quantification of siRNA was performed using a TQ-XS triple quadrupole MS (Waters) coupled to a ACQUITY Premier System LC (Waters). Samples were

| Peptide fragment | Parent m/z | Daughter m/z | Cone voltage (V) | Collision energy (ev) |
|---|---|---|---|---|
| ELLIQFYK y4 | 527.3026 | 585.3031 | 35 | 18 |
| ELLIQFYK y5 | 527.3026 | 698.3872 | 35 | 18 |
| ELLIQFYK y4 HEAVY | 531.3097 | 593.3173 | 35 | 18 |
| ELLIQFYK y5 HEAVY | 531.3097 | 706.4014 | 35 | 18 |
| VLQPPSILYGGR y8 | 650.3746 | 862.4781 | 35 | 23 |
| VLQPPSILYGGR y9 | 650.3746 | 959.5309 | 35 | 23 |
| VLQPPSILYGGR y8 HEAVY | 655.3787 | 872.4864 | 35 | 23 |
| VLQPPSILYGGR y9 HEAVY | 655.3787 | 969.5392 | 35 | 23 |

**Table 2.7:** All transitions monitored during analysis of Ago2. Fragments marked "HEAVY" are generated by SIL IS peptides

injected on a ACQUITY Premier Oligonucleotide C18 Column, 130Å, 1.7 um, 2.1 x 100 mm (Waters, Catalog no. 186009485) held at 60 °C.
The mobile phase consisted of: A: deionized water containing 2.5% hexafluoro-2-propanol (ThermoFisher, Catalog no. H042425G) and 0.105% triethylamine (Sigma-Aldrich, Catalog no. 471283-100ML). B: methanol. The gradient used is shown in Table 2.8. Flow rate was 0.3 ml/min

| Time (min) | %A | %B |
|---|---|---|
| 0 | 95 | 5 |
| 1 | 95 | 5 |
| 4 | 85 | 15 |
| 10 | 70 | 30 |
| 10.5 | 20 | 80 |
| 12.5 | 20 | 80 |
| 12.7 | 95 | 5 |

**Table 2.8:** Gradient used during LC-MS analysis of siRNA

The tool compound siRNA SOD1 was used in all experiments. Length of the sense and antisense strands were, respectively, 21 and 22 nucleotides while the molecular weights of the same were 7012.593 and 7775.149. MALAT1 LNA oligo was used as IS.
The monitored transitions are found in Table 2.9. Transitions for MALAT1 were selected based on previous work. Parent m/z for SOD1 were selected based on full scan data over all values. Selection of daughter m/z as well as values for the cone voltages and the collision energies was performed automatically using the IntelliStart function of the MS system.

| Molecule and charge state | Parent m/z | Daughter m/z | Cone voltage (V) | Collision energy (eV) |
|---|---|---|---|---|
| MALAT1, 7- | 764.466 | 320.7945 | 58 | 30 |
| MALAT1, 8- | 892.0383 | 869.5577 | 48 | 12 |
| SOD1 - AS, 10- | 776.43 | 762.84 | 50 | 14 |
| SOD1 - AS, 9- | 862.79 | 847.72 | 66 | 16 |
| SOD1 – S, | 754.7 | 95 | 56 | 68 |
| SOD1 – S, | 754.7 | 696.54 | 56 | 18 |

**Table 2.9:** Transitions monitored during quantification of siRNA. AS = antisense strand, S = sense strand.

### 2.2.3 Data Analysis

The final data analysis was performed using either Skyline (Pino et al., 2020), TargetLynx (Waters). Data visualization was performed using GraphPad Prism 9 (GraphPad Software).
Standard curves were generated using linear regression using GrapPad Prism 9
When mentioned, “response” refers to the area under the peak of a transition divided by the area under the peak for its corresponding internal standard, as calculated using TargetLynx.

# 3

# Results and Discussion

## 3.1 Selection of Surrogate Peptides

The inital phase of the project can broadly be divided into two parts: the selection of surrogate peptides to quantify in place of the intact Ago2 and the characterisation of candidate antibodies.
The search for an appropriate surrogate was based on recombinant protein instead of the endogenous variant as this significantly lowers the complexity of the samples to be analyzed. A search for vendors of recombinant proteins was performed, leading to the selection of three recombinant human Ago2 (ActiveMotif, OriGene, Sinobiologcal) and one recombinant mouse Ago2 (SinoBiological).
As described in the methods and materials section, the sequence for the mouse variant of Ago2 was first downloaded in a FASTA file format and imported into Skyline which subsequently generated predicted sequences for all tryptic peptides. These were filtered based on length, amino acid content and the presence of motifs that might interfere with downstream enzymatic digestion. The peptides that were retained were of 6-22 amino acids in length and did not contain methionine, cystein or tryptophan, or any repeated stretches of lysine or arginine.
The process was repeated for the human variant of Ago2. As the peptides that remained after filtering were of the same sequence as those for the mouse variant it was assumed that any surrogate peptides that were identified as suitable for the quantification of one variant would also be suitable for the other variant. As such, the human protein was selected for further analysis using high resolution mass spectrometry. The data from this analysis was imported into Skyline to identify which peptide had generated the highest signal. The peptides were ordered based on the summed up peak area for all charge states of the parent ion, the results of which are seen in Table 3.1.
An SRM method for analysis of the two daughter ions that generated the strongest signal was then generated with collision energies and cone voltages were predicted using Skyline. The method can be seen in Table 3.2. Note that several transitions were not chosen based on the data above, instead being included based on previous work.
Hereafter, in cases where specific peptides are referred to, they are done so by the first four amino acids in their sequence. For example, VLQPPSILYGGR is referred to as “VLQP”.

| Peptide sequence | Two strongest daughter ions | Parent mass | Daughter mass |
|---|---|---|---|
| VLQPPSILYGGR | y9 | 650.375 | 959.531 |
| | y8 | | 862.478 |
| ELLIQFYK | y5 | 527.303 | 698.387 |
| | y4 | | 585.303 |
| DYQPGITFIVVQK | y10 | 754.411 | 1101.667 |
| | y7 | | 834.508 |
| AVQVHQDTLR | y6 | 583.8175 | 769.3951 |
| | y5 | | 632.3362 |
| SVSIPAPAYYAHLVAFR | y12 | 931.5016 | 1378.7266 |
| | y10 | | 1210.6368 |
| SGNIPAGTTVDTK | y9 | 630.8251 | 889.463 |
| | y7 | | 721.3727 |
| QFHTGIEIK | y7 | | 797.4516 |
| | y6 | 536.7929 | 660.3927 |

**Table 3.1:** Amino acid sequences of candidate surrogate peptides and which daughter ion generated the strongest signal. Sorted based on the total peak area for the entire peptide as calculated by Skyline

| Peptide and daughter ion | Parent mass | Daughter mass | Cone voltage (V) | Collision energy (ev) |
|---|---|---|---|---|
| TQIFGDR y4 | 418.717 | 494.236 | 35 | 14 |
| TQIFGDR y5 | 418.717 | 607.32 | 35 | 14 |
| SFTEQLR y5 | 440.73 | 646.352 | 35 | 15 |
| TPVYAEVK y5 | 453.75 | 609.324 | 35 | 16 |
| TPVYAEVK y6 | 453.75 | 708.393 | 35 | 16 |
| ELLIQFYK y4 | 527.303 | 585.303 | 35 | 18 |
| ELLIQFYK y5 | 527.303 | 698.387 | 35 | 18 |
| SGNIPAGTTVDTK y9 | 630.825 | 889.463 | 35 | 22 |
| VLQPPSILYGGR y8 | 650.375 | 862.478 | 35 | 23 |
| VLQPPSILYGGR y9 | 650.375 | 959.531 | 35 | 23 |
| DYQPGITFIVVQK y7 | 754.411 | 834.508 | 35 | 27 |
| DYQPGITFIVVQK y10 | 754.411 | 1101.667 | 35 | 27 |
| SIEEQQKPTLDSQR y3 | 829.921 | 390.21 | 35 | 30 |
| SIEEQQKPTLDSQR y7 | 829.921 | 816.421 | 35 | 30 |
| SIEEQQKPTLDSQR y8 | 829.921 | 944.516 | 35 | 30 |
| NTYAGLQLVVVILPKG y10 | 843.003 | 1065.703 | 35 | 30 |
| NTYAGLQLVVVILPKG y12 | 843.003 | 1235.809 | 35 | 30 |

**Table 3.2:** SRM method containing transitions for candidate surrogate peptides

## 3.2 Screen of Antibodies and Detergents

### 3.2.1 Literature Search for Reagents

The next step was to search for and evaluate the detergents and antibodies that would be used in the extraction. The purpose of the antibody screen was to determine what antibody would be suitable to use by looking at the total extraction of recombinant Ago2 protein in buffer, as well as to see how they perform in the presence of the various detergents that would later be used to homogenise various organs and extract the RISC.
By searching through the literature and antibody databases the candidates shown in Table 2.1 were identified. The antibodies were selected based on being monoclonal and reactive in human and mouse. With one exception, they were all supposedly specific to Ago2 and none of the other Ago proteins. It is notable that there exists a significant degree of homology of around 80%, as calculated with sequence alignment using UniProt, between the four Ago proteins, meaning that unless an antibody has been tested and confirmed to be specific to Ago2 it might be cross reactive. In one publication the clone 2E1C-1C9 displayed cross reactivity with all four Ago protein in mouse (Pei et al., 2010). Since there exists a large degree of homology of 99.3% between human and mouse Ago2 the supposedly human specific clones 11A9 and 4G8 were included as well.
It is worth noting that antibodies were included in the experiments as they arrived from their suppliers, meaning that earlier experiments might not include all antibodies that later ones do. Additionally, the analyses were performed on several different instruments, meaning that the magnitudes of the peak areas may vary from experiment to experiment. Comparisons should be made within individual experiments, not between them.
An additional literature search was performed to identify what lysis buffers have previously been used to extract RNA-protein complexes in general, and RISC more specifically. Focus was placed on identifying what detergents were used as these were assumed to have to greatest impact both on the total extraction of protein during homogenisation but also to have the greatest impact on the ability of the antibodies to extract the protein. The publications in this search used NP40 (Zhou et al., 2012), Triton X-100 (Cristea & Chait, 2011; Pei et al. 2010) (Triton), and Tween-20 (Tween) (Cristea & Chait, 2011) as their detergents of choice. Sodium dodecyl sulphate (SDS) was generally not used but was also selected as a candidate detergent to use due to its ability to denature protein. This could possibly have assisted in extraction if Ago2 is associated with components of the tissue homogenate that can interfere with the ability of the antibodies to capture it (Andersen et al., 2009; Zhou et al., 2012). NP40 and Tween were acquired as pure detergents and dissolved at 1% by volume in PBS while Triton and SDS were acquired in the form of the pre-blended lysis buffers RIPA and MSD Tris lysis buffer (Meso Scale Discovery).

### 3.2.2 Proof of Concept

The first experiments served as a proof of concept to see whether the antibodies were able to extract Ago2. Immunoprecipitation (IP) was performed in tris buffer according to the described method using the clones JF0992 and 11A9 with two human Ago2 variants from ActiveMotif and OriGene as well as the one mouse variant SinoBiological. To serve as a control recombinant protein was also subjected to digestion with trypsin/Lys-C without first undergoing IP. Each condition was tested in duplicate. 5.2 µl of slurry was used during to perform IP and samples were diluted five times before incubation.
Samples were analysed using TQ-MS with the conditions previously described. By looking at the peak areas for the four strongest transitions (Figure 3.1) several things can be read.
First, the transition of the y9 ion for the peptide VLQP was generally the strongest transition, making VLQP potentially the most suitable to act as a surrogate peptide.
Second, the peptide SGNI does not appear to generate a signal the protein from OriGene is analysed. The fact that the remaining peptides all appear to generate a signal indicates that the OriGene protein might not be complete in sequence, an idea which is strengthened by the fact that the peptide SGNIP is close to the C-terminal of the protein, being composed of amino acids 726 to 738 in the human variant.
Third, 11A9 generally outperforms JF0995 in the total extraction.
As the peak areas of the controls represent the theoretically maximum value that can be achieved it is also of interest to look at the fraction between the peak areas of the controls and that of a sample that has undergone IP. This value serves as a measure of the efficiency of the extraction.
Looking at the calculated efficiencies (Figure 3.2), extraction seemingly depends on what peptide on is looking at as it varyies from above 80% to below 40% for the pair 11A9:OriGene. While strange, there are reasons for this to occur. As the IP is performed using streptavidin coated beads and antibodies it is possible that something coelutes with some of the peptides and causes signal suppression. The difference in extraction efficiencies between the protein from Active Motif and that from SinoBiological was also notable. While the extraction efficiency was roughly equal for JF0992, for 11A9 the extraction of SinoBiologicals protein was around half that of Active motifs protein. The this could be explained by the specificity of the antibodies used in this experiment. As shown in Table 1, 11A9 was stated to be specific to human Ago2 while JF0992 was stated to be cross-reactive with mouse and human Ago2. As Active Motifs Ago2 was of the human variant and SinoBiologicals was of the mouse variant it could be that 11A9 indeed does show a preference for human Ago2 over mouse Ago2.
The experiment was repeated once more to study if the response of the extraction was linear. Human (OriGene) and mouse (SinoBiological) Ago2 was diluted in PBS at five concentrations: 2000, 500, 125, 31.25 and 7.8 ng/ml. IP was then performed using clones 11A9 and JF0992. Two samples at 2000 ng/ml of each protein were also subjected to digestion without undergoing IP to serve as controls. Linear regression was used to generated curves which used to study the linearity of extraction (Figure 3.3). For the pairing 11A9:Mouse (Figure 3.3 b)) the point at lowest concentration generated a seemingly unproportional response, leading to a

poor fit of the curve. Excluding it (Figure 3.3 c)) generates a more well-fitted curve. Looking at the human protein, 11A9 again appears to outperform JF0992 while the extraction of mouse Ago2 is roughly equal. In either case the response appears to be linear over the span of concentrations tested.

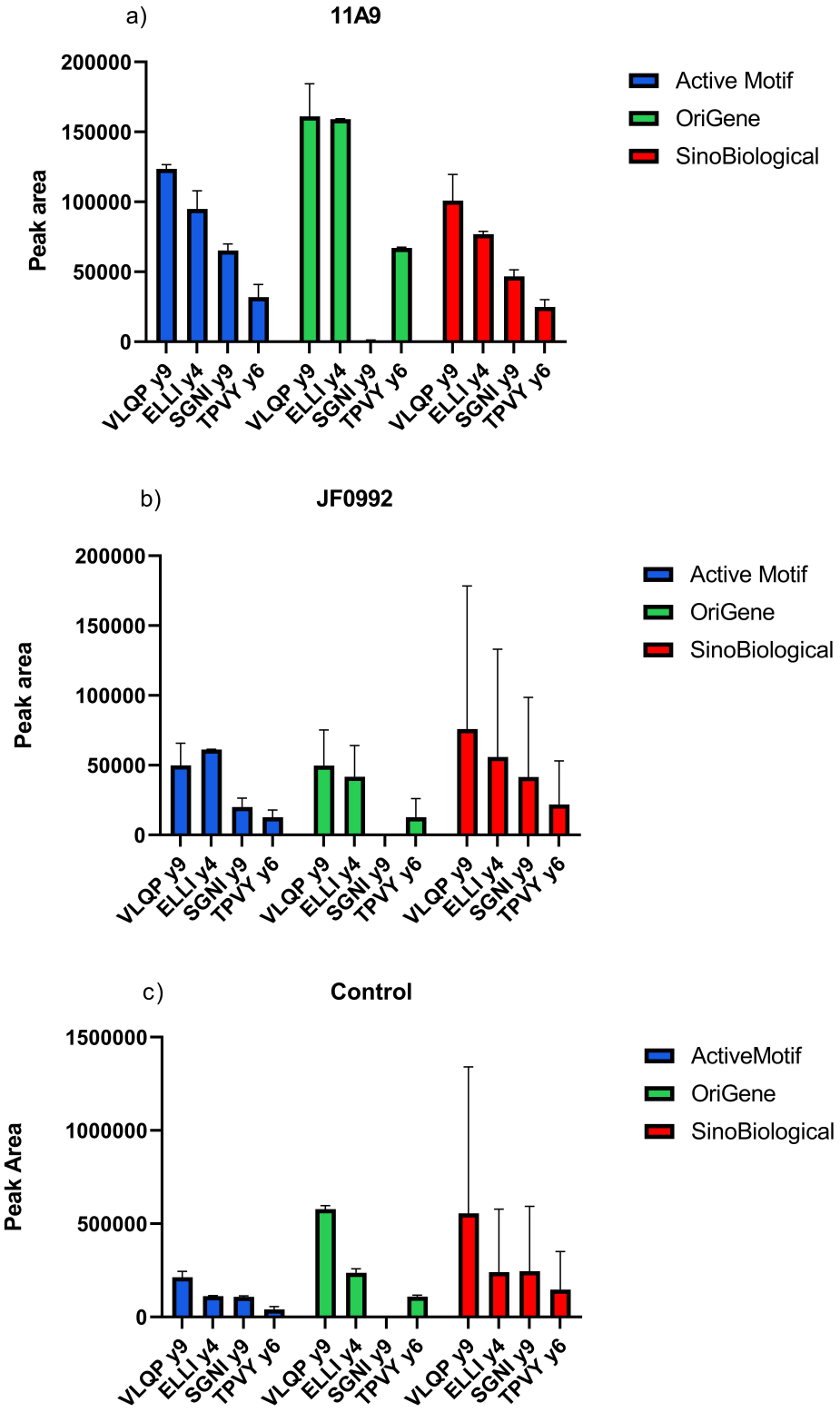


**Figure 3.1:** Mean peak areas with standard deviation for the four strongest surrogate peptides from three different recombinant proteins after immunoprecipitation with antibodies 11A9 (a) and JF0992 (b) with digested recombinant protein used as a control (c). Peptide sequences have been abbreviated.

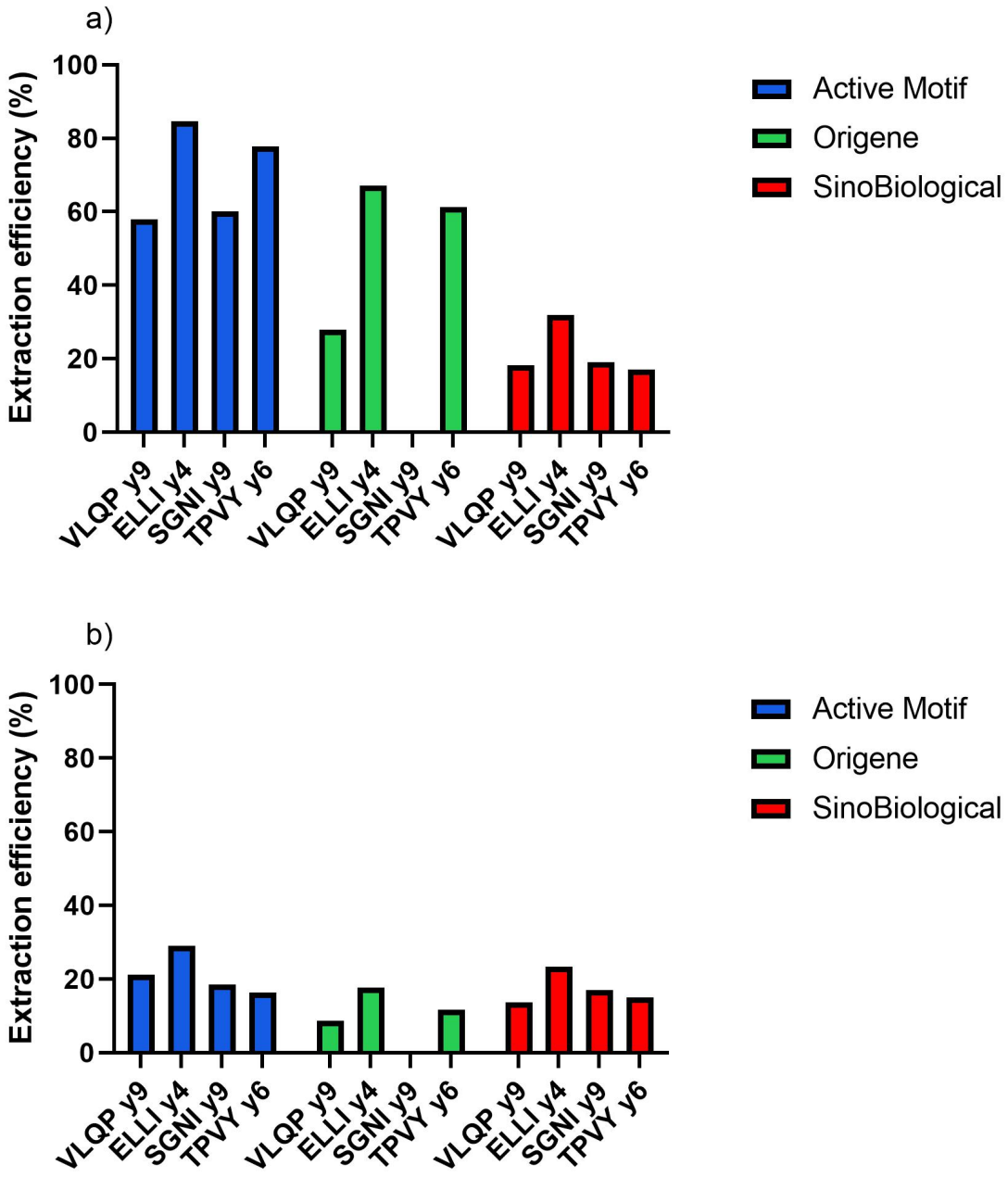


**Figure 3.2:** Extraction efficiencies of recombinant Ago2 for antibodies a) 11A9 and b) JF0992. Extraction efficiency of protein from OriGene as calculated from peptide SGNI has been excluded.

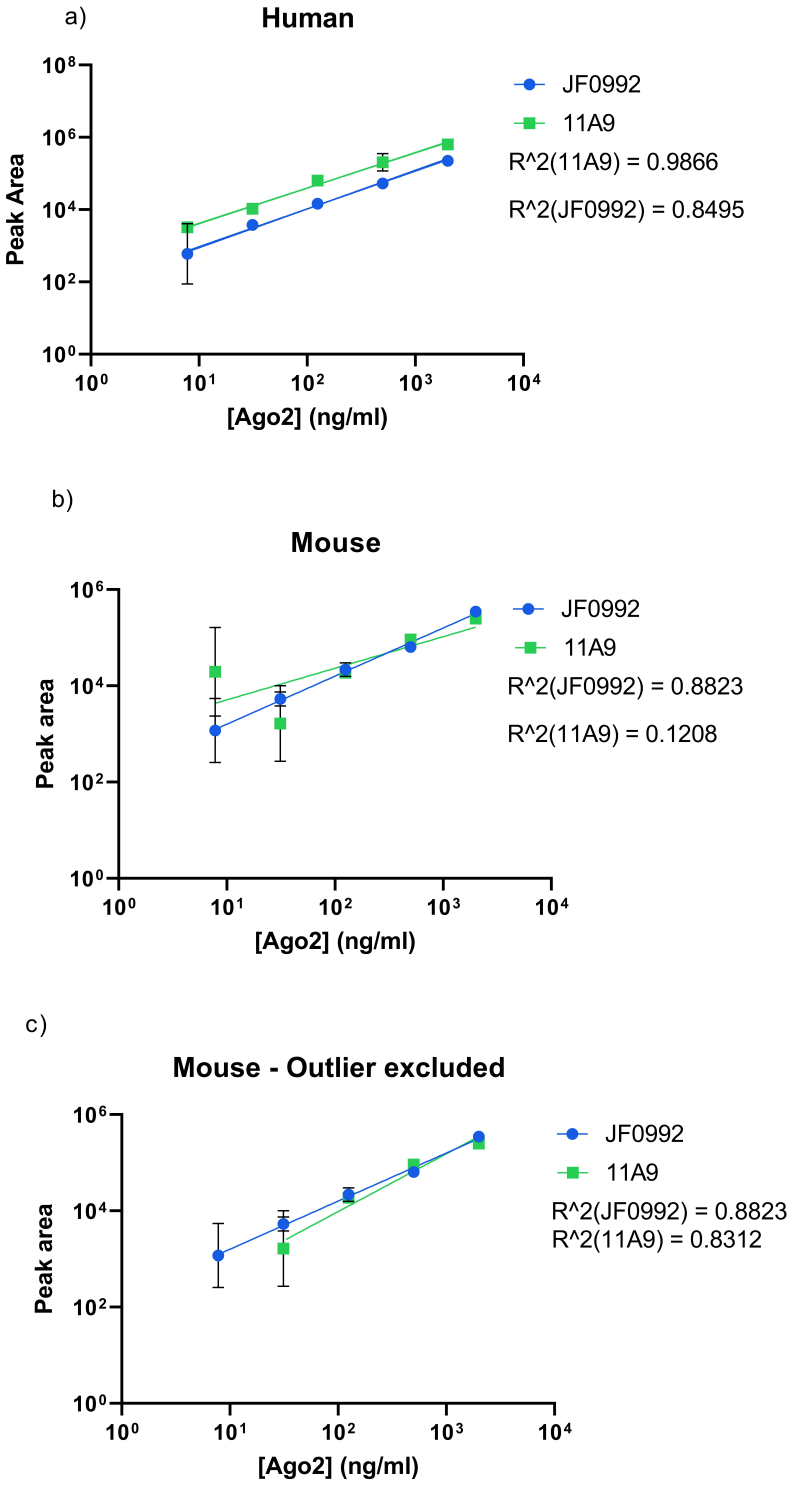


**Figure 3.3:** Mean values with standard deviation of log10 transformed peak areas of transition VLQP y9 versus the log10 transformed sample concentrations. a) Plot for human Ago2. b) Plot for mouse Ago2. c) Plot for mouse Ago2 with point at lowest concentration for 11A9 excluded.

### 3.2.3 Studying the Effects of Detergents on Immunoprecipitation

After the initial proof of concept showed that the method was viable to extract Ago2 from buffer, a possible concern arose that the detergents might interfere with the extraction of Ago2 during immunoprecipitation. To study these effects, experiments were performed to measure the extraction of recombinant protein that had been dissolved in solutions containing the various detergents that would later be used in the homogenisation of tissues.
A first experiment tested the influence of NP40 and Tween on the extraction of human (OriGene) and mouse (SinoBiological) Ago2. The proteins, at a concentration of 500 ng/ml, were diluted in 1% solutions of NP40 or Tween in PBS. IP was then performed using the antibodies 11A9, 2D4, 4G8 and Monoclonal Rabbit IgG Clone #036 (#036). Due to clone JF0992 performing similarly or worse than 11A9 in previous tests it was excluded.
For a given antibody, the extraction of human Ago2 appeared to be generally similar between the detergents (Figure 3.4). The one exception being for antibody #036 where the extraction of mouse protein was significantly higher in Tween than in NP40.
The process was repeated to test the impact of SDS and Triton by performing IP of mouse Ago2 (SinoBiological) in RIPA and MSD tris lysis buffers, respectively. The antibody clones 11A9, #036, 2D4 and ab57113 were tested. IP was also performed in pure tris buffer without any detergent to serve as control. The extraction in MSD was similar to that in pure tris buffer while the extraction in RIPA was much lower (fig. 5). For antibodies 2D4 and ab57113 the deviation between duplicates is significantly higher in MSD and Tris as compared to RIPA. As this effect was only seen in two of the antibodies this is most likely due to some complication that occurred during the handling of the beads after incubation, such as losses from pipetting during the repeated washes.
While RIPA seemingly had the lowest extraction of Ago2 in very pure systems composed of buffer and recombinant protein alone, it was thought that this might not be reflective of how it would affect homogenised tissues. In a more complex system, it was possible that a stronger detergent would be more beneficial for extraction as it might dissociate components of the matrix that might interfere with the binding of the antibody to the epitope. However, simultaneously the detergent must not be so strong that it denatures Ago2 as this could lead to the loss of the bound siRNA.
In addition to how they influenced the immunoprecipitation of Ago2 it was of interest to measure how effectively the detergents could extract protein from the homogenised tissue. A BCA assay was performed to measure the total protein concentration homogenates of mouse liver tissue containing the three detergents.
Blank tissue was homogenised at a ratio of 100 µg of tissue to 900 µl of lysis buffer. The three homogenates were diluted 100 times before analysis. The total protein concentrations of the three homogenates were measured to be 24.1 mg/ml for MSD, 20.0 mg/ml for RIPA and 15.5 mg/ml for Tween. Using this value as a surrogate to the amount of Ago2 that could potentially be extracted, MSD and RIPA buffer were selected for further development.

Finally, due to the high variability in several of the cases the thought arose that the Tween used in the wash steps of the extraction might be interfering with the extraction. Antibody 11A9 was thus incubated with human recombinant protein at three concentrations and washed as described. The initial two washes were performed with pure PBS, PBS with 0.01% Tween or PBS with 0.05% Tween. The remaining washes were performed as previously described.
The peak areas appear to be essentially the same regardless of the presence of detergent (Figure 3.6). The fact that the variability was the highest at the 10 ng/ml level could be due to a high signal to noise ratio hindering accurate measurement of the sample.
As a summary, it appeared that the detergents to be used in the homogenisation of tissue could influence the extraction of Ago2 during IP. As Ago2 was successfully extracted in all cases it did, however, appear that the chosen candidates were suitable for further testing in homogenised tissue. NP40 was discarded as an option based on the substantially higher extraction of mouse protein by antibody #036 in Tween (Figure 3.4). Similarly, the antibodies performed differently enough that further testing would be necessary to determine which one would be used in the final assay.

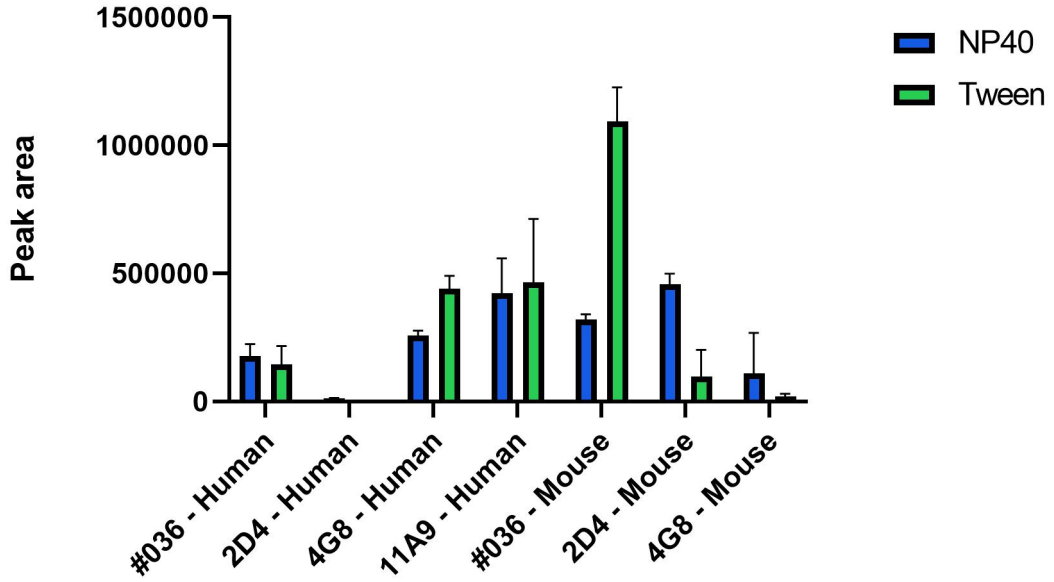


**Figure 3.4:** Mean peak areas with standard deviation after immunoprecipitation of human and mouse Ago2 in 1% solutions of NP40 or Tween in PBS.

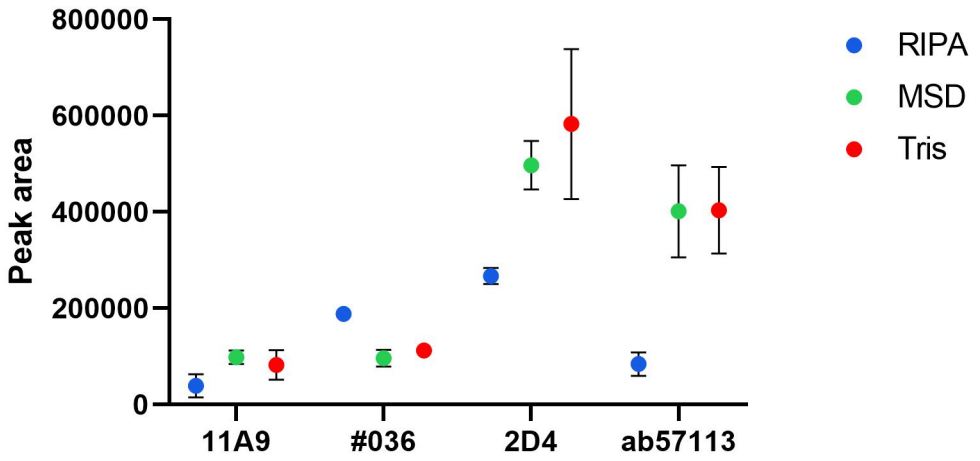


**Figure 3.5:** Mean peak areas and standard deviations of duplicates for VLQP y9 after immunoprecipitation in RIPA and MSD lysis buffers as well as in tris buffer.

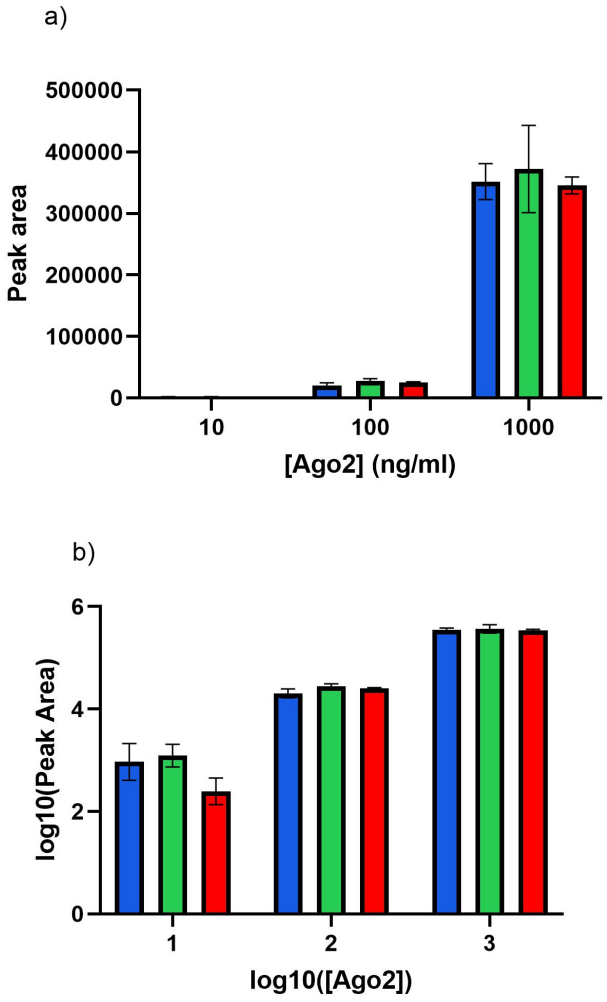

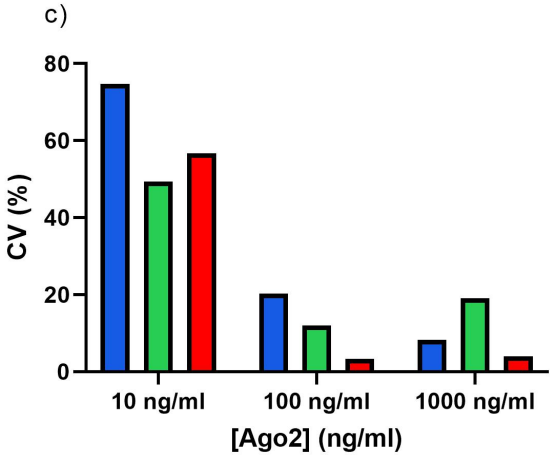


**Figure 3.6:** Results for washes with PBS containing 0% (blue), 0.01% (green) or 0.05% (red) Tween. a) Mean peak areas with standard deviation for transition VLQP y9. b) Log10 transformed data from a). CV values for each tested condition

### 3.2.4 Evaluation of Antibodies in Homogenate

The tests were extended to include homogenised mouse tissue as well. Under the assumption that differences between different tissues would be minor, only liver was initially studied.
IP was performed on mouse liver tissue that had been homogenised as described above using either RIPA or MSD lysis buffer. These experiments would also be used as a basis to select the best candidate surrogate peptides.
In a series of experiments, all antibodies were screened to measure their extraction efficiency of Ago2. Initially all antibodies except 2E1C-1C9 were tested.
Recombinant human protein (OriGene) was subjected to digestion in 50 mM Tris buffer to serve as control. Clone 2E1C-1C9 was tested in the same manner in a separate experiment. At this point IS peptides were also available and were therefore included in the analysis.
By comparing the retention times displayed in the chromatograms (Figure 3.7 it seems that none of the transitions generated by analysing the control appear during analysis of samples underwent IP, indicating that Ago2 was either not successfully extracted from the homogenate or extracted at levels too low to measure with the instruments setup that was used. However, in samples where antibody 2E1C-1C9 was used the elution times for the peptides VLQP and ELLI are the same as for their heavy SIL variants, 3.43 and 3.60 minutes, respectively (Figure 3.8.
As 2E1C-1C9 appeared to be the only antibody which, under the tested conditions, successfully extracted Ago2 at a detectable level it was selected to be used in the later optimisation of the immunoprecipitation conditions.

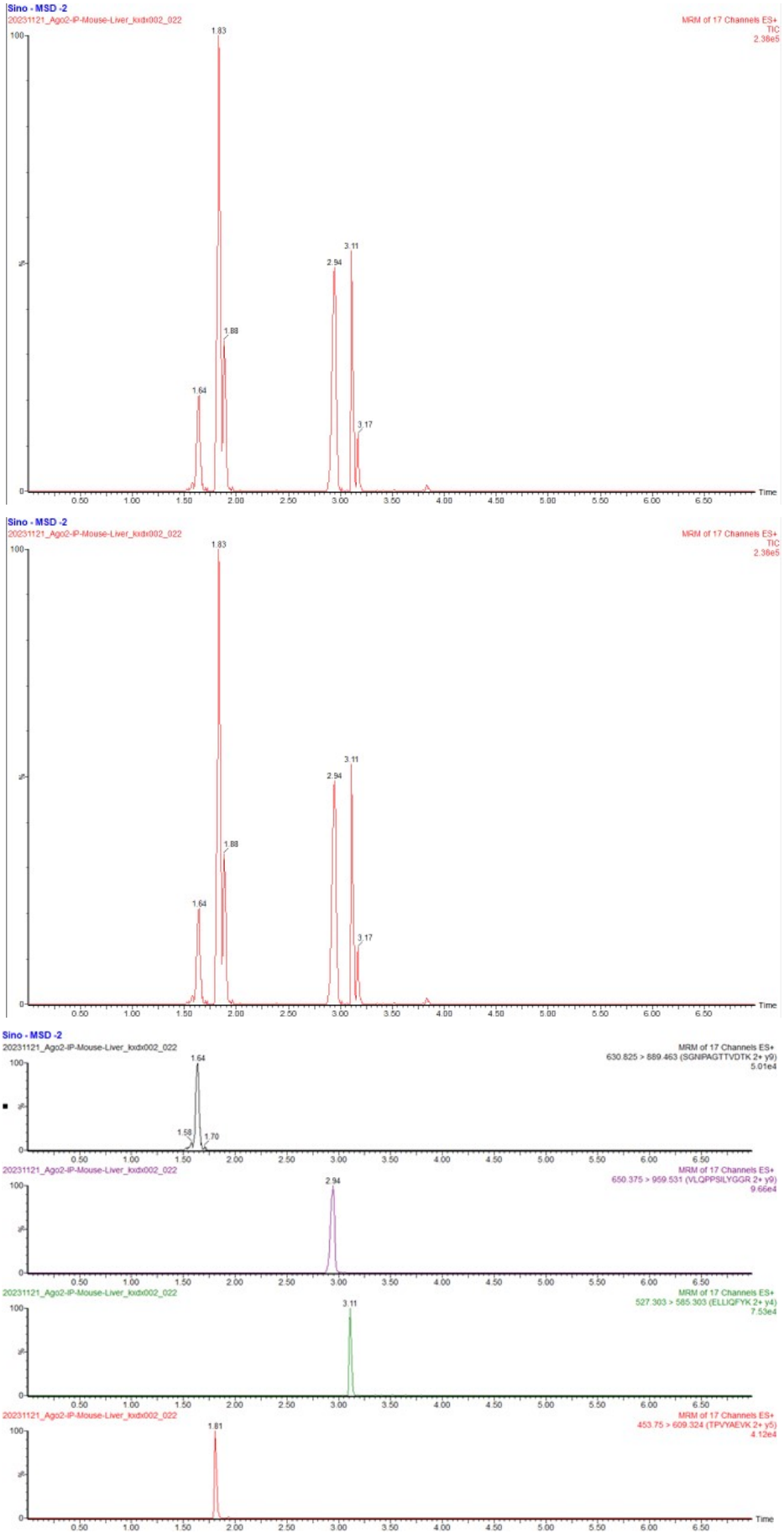
Sino - MSD -2
20231121_Ago2-IP-Mouse-Liver_kxdx002_022
MRM of 17 Channels ES+
TIC
2.36e5
1.83
3.11
2.94
1.88
1.64
3.17
Time
Sino - MSD -2
20231121_Ago2-IP-Mouse-Liver_kxdx002_022
MRM of 17 Channels ES+
TIC
2.36e5
1.83
3.11
2.94
1.88
1.64
3.17
Time
Sino - MSD -2
20231121_Ago2-IP-Mouse-Liver_kxdx002_022
MRM of 17 Channels ES+
630.825 > 889.463 (SGNIPAGTTVDTK 2+ y9)
5.01e4
1.64
1.58
1.70
20231121_Ago2-IP-Mouse-Liver_kxdx002_022
MRM of 17 Channels ES+
650.375 > 959.531 (VLQPPSILYGGR 2+ y9)
9.66e4
2.94
20231121_Ago2-IP-Mouse-Liver_kxdx002_022
MRM of 17 Channels ES+
527.303 > 585.303 (ELLIQFYK 2+ y4)
7.53e4
3.11
20231121_Ago2-IP-Mouse-Liver_kxdx002_022
MRM of 17 Channels ES+
453.75 > 609.324 (TPVYAEVK 2+ y5)
4.12e4
1.81
Time

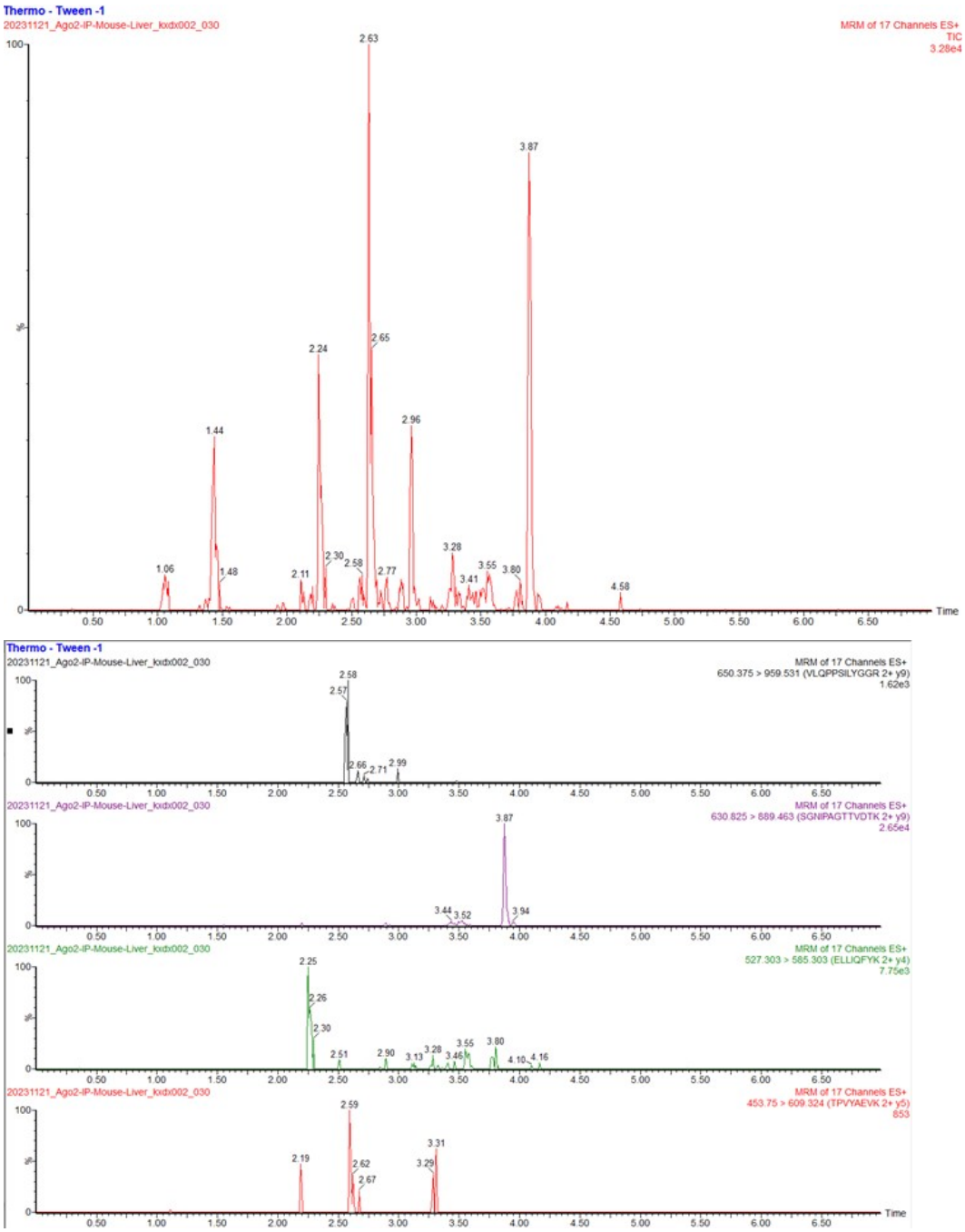


**Figure 3.7:** Showing TICs and chromatograms of the four strongest transitions for digested recombinant human Ago2 (top two) and corresponding chromatograms for liver homogenate homogenised using MSD and subjected to IP using antibody 2D4 (bottom two). Remaining chromatograms can be seen in Appendix 1 and appear similar. Note that experiment names in upper right are incorrect due to an error in the setup of the analysis.

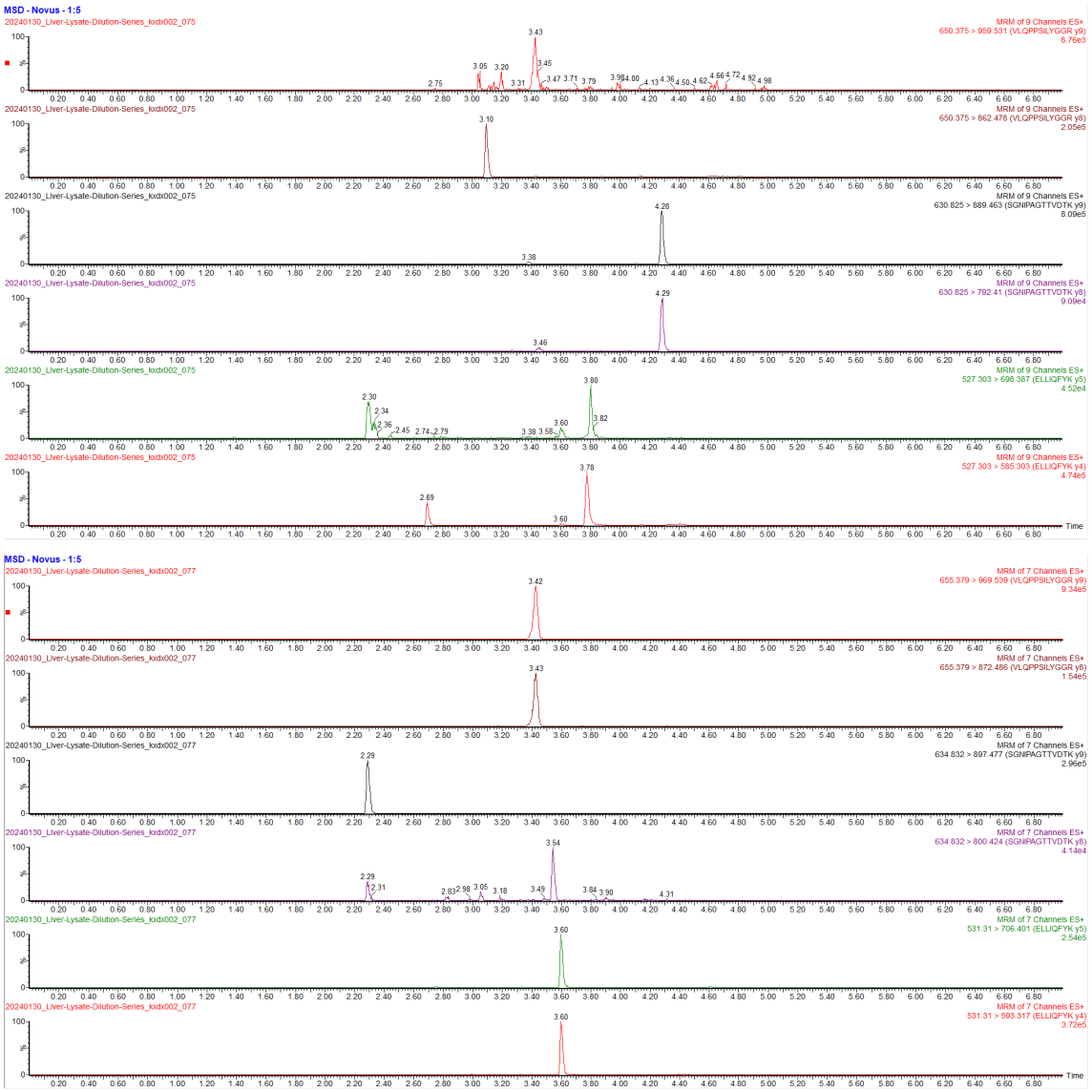


**Figure 3.8:** Transitions of peptides (top) generated after digest of homogenate that had been homogenised using MSD and subjected to IP using clone 2E1C-1C9, and SIL peptides spiked into the same sample after work-up (bottom)

## 3.3 Optimising Extraction Conditions

The next step in the development of the assay was to optimise the extraction process. The end goal was to have an assay with a high and consistent extraction of RISC. In addition to this, as the amount of extracted siRNA was assumed to be proportional to the amount of Ago2, only the latter was quantified for much of the development.

### 3.3.1 Evaluating the Effects of Increasing Antibody Concentration

Having chosen an antibody to use, the next question was how much of the antibody should be used. Two parameters influence this: how much of the antibody that is conjugated to the magnetic beads used for the extraction as well as how much of the resulting slurry that is added to a given sample. Both of parameters were studied.
Previous experiments added 5.2 µl of bead slurry to 50 µl of liver homogenate that was then diluted five times by adding 200 µl of Tris containing 0.1% BSA. To evaluate how much the amount of added slurry affects the extraction, an experiment was conducted where 5.2 µl of slurry was tested along with 10 µl. In addition, 50 µl of human recombinant protein (ActiveMotif) diluted in 50 mM Tris-HCl to a final concentration of 40 and 200 ng/ml was spiked into the samples to determine if the extraction was linear with respect to the concentration of Ago2 in the sample. To ensure that all samples were incubated at the same volume only 150 µl of Tris BSA was added to spiked samples.
Doubling the amount of slurry leads to a proportional doubling of the response in all samples (Figure 3.9). However, the variation appeared to be higher at higher concentrations of Ago2 when more bead is used. Spiking in 40 ng/ml of protein did not appear to generate a measurably larger response while spiking in 200 ng/ml did, likely due to that the added concentration compared to the endogenous levels was low and could not be detected
From the experiments it appeared that increasing the amount of slurry added to a given sample could significantly increase the extraction. To examine if the trend held and that doubling the amount of slurry again would double the response and additional experiment was performed were 20 µl of slurry was added to homogenate that had been diluted as previously described to reach a final dilution factor of 5, 25, and 125. 0, 3.125, 12.5 and 25 ng of recombinant Ago2 (ActiveMotif) was spiked into the samples by adding 50 µl of 62.5, 250 or 500 ng/ml of recombinant Ago2 diluted in 50 mM of tris.
As comparison, 10 µl of slurry was also added to homogenate at a final dilution of 25 times, into which 0 and 3.125 ng of recombinant Ago2 was spiked. Analysis was performed using a TQ-Absolute MS system coupled to a Premier LC system.
The response continued to increase with more added slurry and, predictably, the less diluted samples generated a higher response (Figure 3.10). However, some strange behaviours can be seen. While the response decreases as the samples are diluted more, it does not do so proportionally. The responses for samples diluted five times is only around two and a half times higher than those diluted 25 times, instead of the five times higher as might be expected.
A second oddity is the fact that at five times dilution the response appears to increase as the concentration of Ago2 is increased until the point were 500 ng/ml of Ago2 is added where it instead sharply drops. It also at this point where the variability of the response is the highest.This appeared to be a consistent effect across runs, as it was visible when the experimental conditions were repeated on two consecutive days at a later date (Figure 3.11
To address this, it became necessary to evaluate potential solutions. A possible

cause that was identified was a loss of the magnetic beads during the wash steps after incubation. To remedy this a new magnet was ordered and tested together with switching to using Nunc plates as they fit more tightly to the new magnet than the Protein LoBind plates that had been used up until this point. This appeared to have been a successful solution to the problem as the response consistently increased as more protein was spiked into the homogenate (Figure 3.12). However, it is unclear why this would be the case as the problem does not appear at a higher dilution factor (Figure 3.10, Figure 3.12). A possible cause is that, by pure chance or systematic experimental error, the loss of beads was the unequally high in the deviating sample as compared to the other samples, leading to a drop in response. If the new magnet eliminated this effect the drop in response would also be eliminated.
Finally, the impact of the amount of antibody per µg of bead was evaluated. In two separate experiments homogenate homogenised using MSD was incubated with 20 µl of slurry with either 4.5 or 9.1 ng antibody per µg bead.
The results of these are inconsistent with each other. In one case (Figure 3.13 a)) the increased antibody concentration leads to an apparent decrease in response while in another (Figure 3.13 b)) the response is either increased or unaltered by the higher concentration of antibody. In either case the variation in several of the points is large, indicating that the extraction was inconsistent.
All optimisation up to this point had used antibody 2E1C-1C9. As previously stated, this antibody had been shown to be cross reactive with all four Ago proteins, not just Ago2. As RISC can be formed from form all the Ago proteins it was decided that antibody 2D4 would be tested again as it had previously been shown to be specific to Ago2. It had also been used to extract RISC in the same publication as had shown the cross-reactivity of 2E1C-1C9. Thus 2D4 was included as part of the same experiment testing the new magnet. Samples where 2D4 was used were spiked with 0 and 250 ng/ml of recombinant Ago2 while samples where 2E1C-1C9 was used were spiked with 0, 125, 250 and 500 ng/ml. The results (Figure 3.14 appear to show that, after improving the extraction conditions, 2D4 performs similarly to 2E1C-1C9. The apparent drop in response with increasing concentration shows that the procedure was still either inconsistent or insensitive to the level of Ago2 in the samples.
In summary, increasing the amount of slurry added to a sample during IP appeared to be a realiable means of increasing extraction. Increasing the amount of antibody per bead did not, in contrast, generate such a clearly better extraction. While it would be possible to continue increasing the amount of slurry used in the extraction, it was decided that using 20 µl struck a balance between a high extraction and the cost of reagents.

### 3.3.2 Screen of Surrogate Matrices

In order to accurately quantify the amount of Ago2 in sample it is necessary to correlate the generated response to a concentration. Commonly this is done using a standard curve where known amounts of the analyte are subjected to the same treatment as the samples themselves. After analysis, linear regression can be used to determine the relationship between the response of the instrument and the

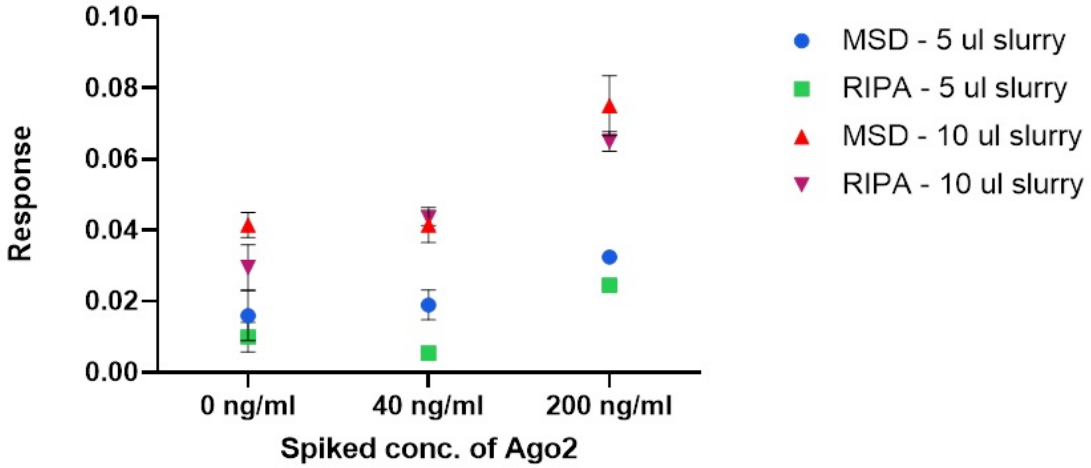


**Figure 3.9:** Mean and standard deviation of responses in homogenate samples spiked with 0, 40 or 200 ng/ml of recombinant Ago2 and subjected to IP with either 5 or 10 µl of bead slurry.

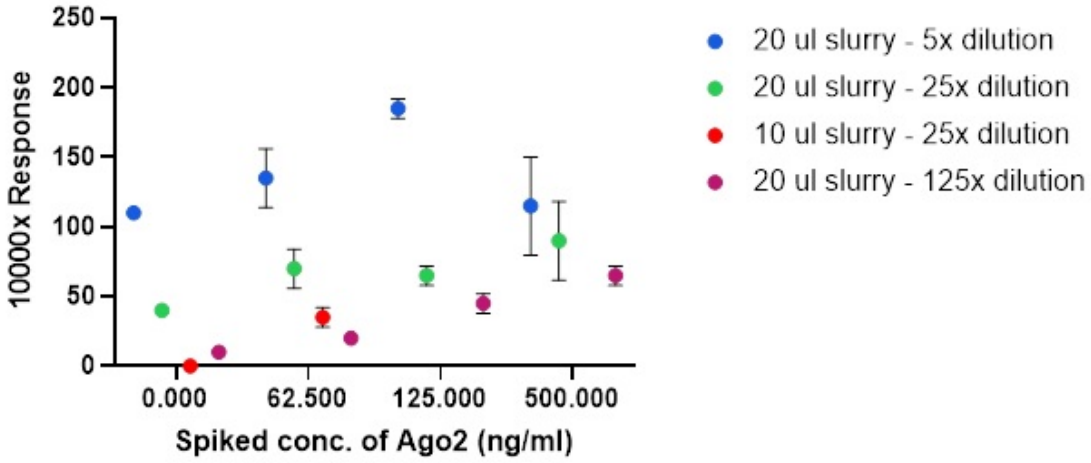


**Figure 3.10:** Results for IP in samples diluted five, 25 and 125 times, with 10 or 20 µl of slurry added and with 0, 62.5, 250 or 500 ng/ml of recombinant protein spiked in to the sample before IP.

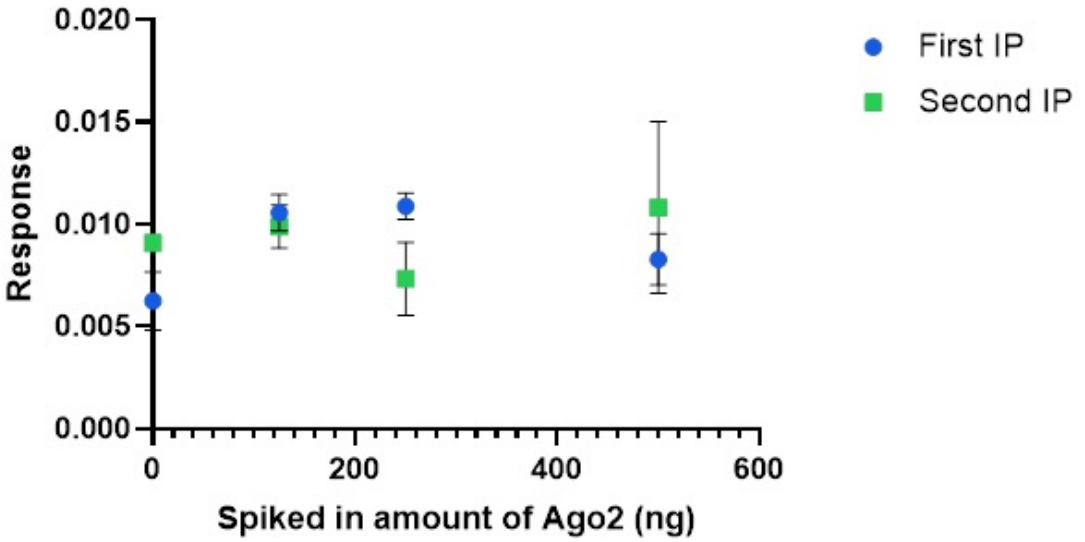


**Figure 3.11:** Mean value and standard deviation of responses measured from IP performed on two consecutive days using 20 µl bead in liver homogenised with MSD lysis buffer.

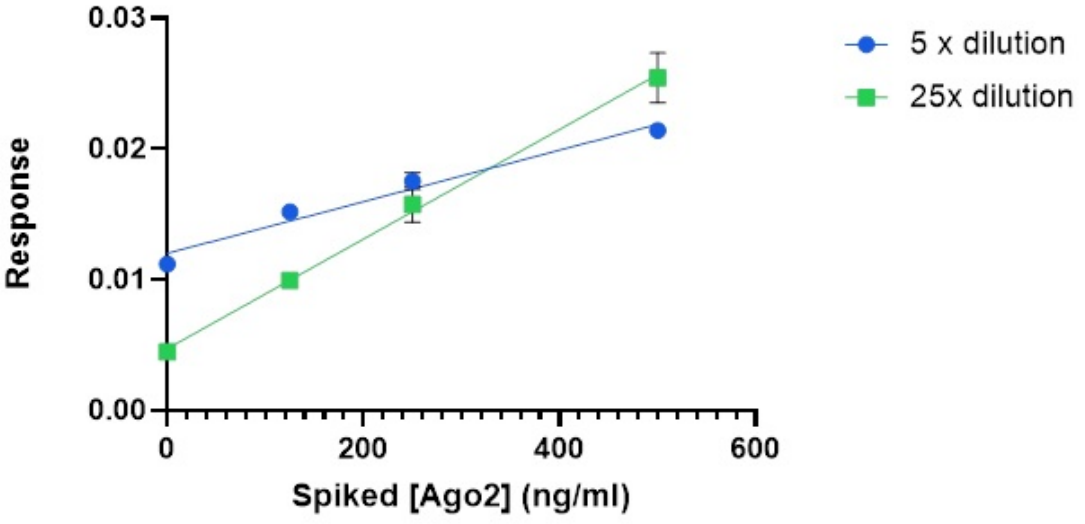


**Figure 3.12:** Mean value and standard deviation of response of IP performed using new magnet, 20 µl slurry in liver homogenised with MSD lysis buffer diluted five or 25 times with tris buffer.

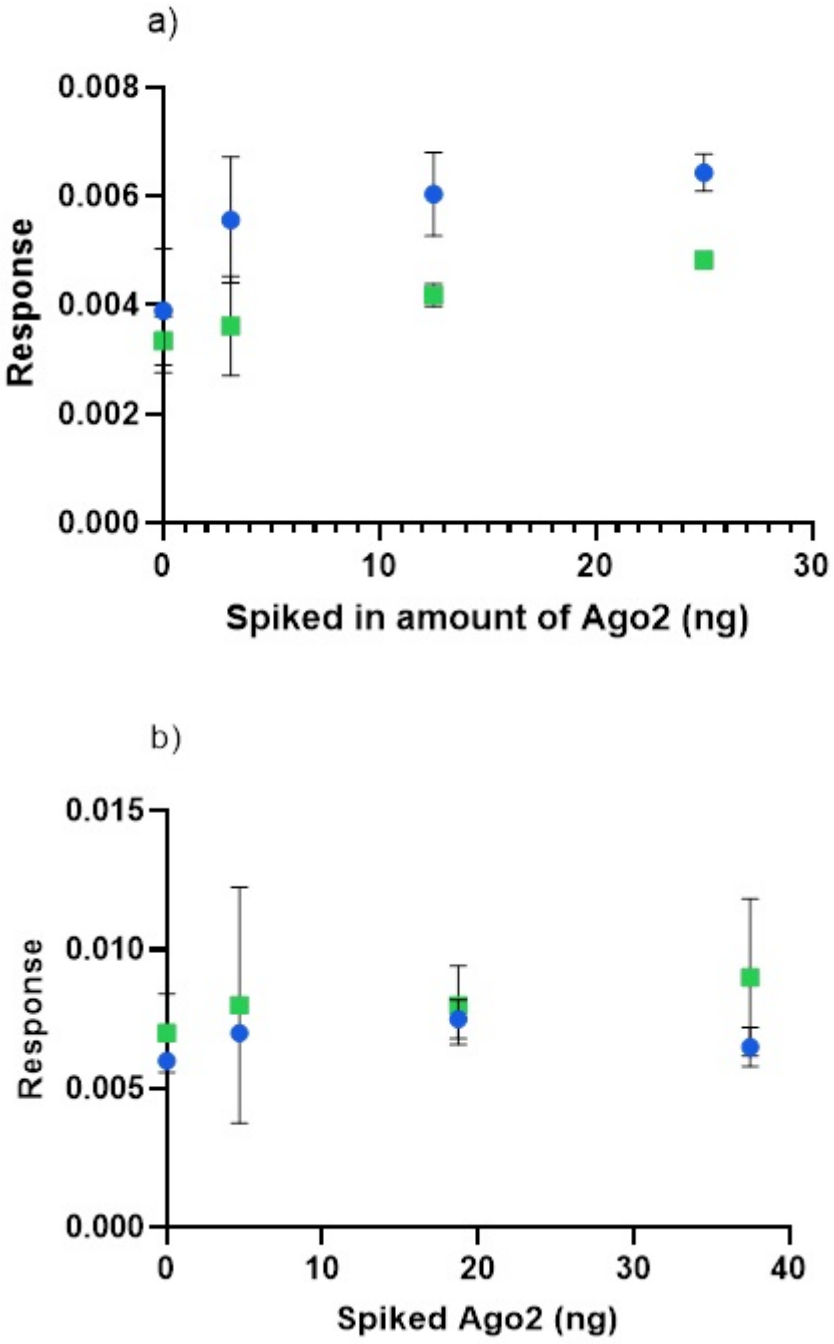


**Figure 3.13:** Mean value and standard deviation of the measured response after IP of liver tissue homogenised with MSD with 20 µl of slurry with 4.5 (blue) or 9.1 (green) ng antibody/µg bead on two separate occasions.

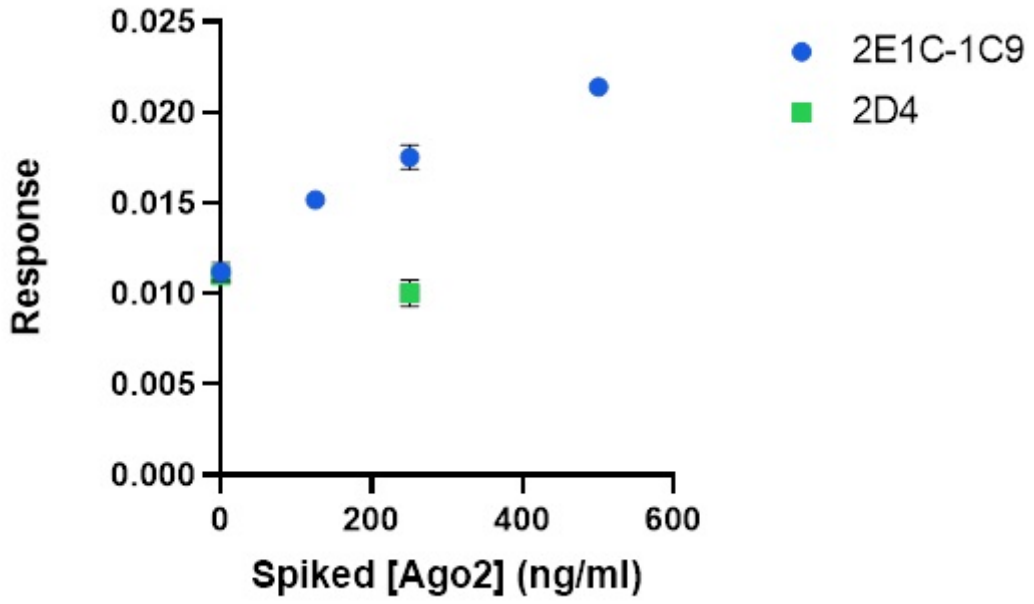


**Figure 3.14:** Mean response with standard deviation of IP performed with antibodies 2D4 or 2E1C-1C9 in liver homogenised with MSD and diluted five times. Data for 2E1C-1C9 has been shown previously.

concentration of the analyte which in turn can be used to estimate the analyte concentration in a sample based on its response.
As the concentration of the points used to construct the curve have to be known for accurate quantification to be possible, the standard curve should be constructed in a blank matrix that does not naturally contain the analyte. Ideally this matrix should be the same as that of the samples, but in cases were the analyte is endogenous this is not possible. While several approaches exist to address this, in this project two approaches were tested. The first of these was the usage of an alternate blank matrix, known as a surrogate matrix, in place of the sample matrix to construct standard curves.
The second was the method of standard addition, where analyte is spiked into the sample matrix various concentrations. By then performing linear regression, the endogenous analyte concentration can be estimated from the x-intercept of the calibration line.
Four potential surrogate matrices were tested: Tris buffer, RIPA and MSD lysis buffers, mouse plasma and mouse plasma diluted with lysis buffer. The approach taken to evaluate the matrices was as follows. Standard curves of Ago2 were constructed in homogenate and the potential surrogate matrices by, respectively, spiking in a series of concentrations of recombinant protein into the homogenate or via serial dilution using a given surrogate matrix. By then plotting the response generated at the various concentrations versus the actual concentrations and performing linear regression, the relationship between the two could be examined. In a suitable surrogate matrix, the slope of the line generated in this manner would be the same as that of the homogenate.

This approach was first applied to RIPA and MSD lysis buffers. Recombinant Ago2 was serially diluted with lysis buffer diluted 25 times with tris buffer according to the scheme in Table 3.3. Homogenates containing lysis buffer were then diluted 25, 50 and 100 times and spiked with 50 µl of recombinant Ago2 in tris at the concentrations 0, 20, 50, 100 or 500 ng/ml. IP was performed, and the samples were analysed using a TQ-XS MS system coupled to a Premier LC system. Note that as this experiment was performed before the effects on the volume of slurry on the response was studied, only 5 µl of slurry was used. The results of this experiment (Figure 3.16) imply that there was significant interference from the homogenate apart from that contributed by the lysis buffers, as for neither buffer do the slopes of the lines match those of the homogenates at any dilution.
In a similar manner, plasma diluted with tris buffer or MSD lysis buffer as well as tris alone were evaluated. Serial dilution of recombinant Ago2 was performed according to Table 2.2 using mouse plasma diluted with tris, with MSD lysis buffer or 50 mM tris-HCl. MSD homogenate was diluted 25 and 100 times and spiked with 50 µl of recombinant Ago2 in 50 mM tris at concentrations 0, 125 and 250 ng/ml. IP was performed using 10 µl of slurry. Here it appeared that both curves that were generated in plasma (fig. 16 a)) were close to those in homogenate while the slope of the curve generated in Tris was much steeper. However, the apparently nonlinear response from the homogenate makes it difficult to make any clear statements about the suitability of plasma as a surrogate matrix. Indeed, in the log transformed data (fig. 16 b)) it appears that the curve generate in homogenate has a steeper curve than either curve in plasma as well as that in Tris.
In the end, none of the potential surrogate matrices appeared to fully match the homogenate. While these experiments were only conducted in liver homogenate it was assumed that the results would be similar if other tissues were tested.
The next option was to use standard addition. This approach was complicated by the fact that in several experiments the response was not linear with respect to the spiked concentration (Figure 3.10, Figure 3.11). However, resolving this, enabled the generation of two standard curves in liver homogenate, one where the homogenate was diluted 5 times and the other where it was diluted 25 times. The curves had x-intercepts of, respectively, -608.3 and -112.2. Correcting for the dilution by dividing the x-intercepts with their respective dilution factors gave calculated concentration of 3050 ng/ml in the 5 times diluted homogenate and 2800 ng/ml in the 25 times diluted homogenate, a difference of 9%.
However, while standard addition appeared to be a possible alternative to determine the concentration of Ago2 it had the drawback of using large amounts of homogenate to prepare the standard curve. As such it was decided that the surrogate matrix approach would be used instead, with the most suitable matrix to construct standard curves in being Tris buffer due to the low cost and ease of handling compared to the plasma-based alternatives. While this limits the assay to providing relative comparisons this was deemed to be sufficient.
In addition to this, as the highest response in homogenate was consistently achieved in five times dilution later experiments would use this.

| Stock (uL) | Diluent (uL) | conc. Ago2 (ng/ml) |
|---|---|---|
| 10 | | 100000 |
| 10 | 490 | 2000 |
| 150 | 350 | 600 |
| 150 | 350 | 180 |
| 150 | 350 | 54 |
| 150 | 350 | 16.2 |
| 150 | 350 | 4.86 |
| 150 | 350 | 1.458 |
| 0 | 400 | 0 |

**Table 3.3:** Dilution series used to generate standard curve for testing of lysis buffers as surrogate matrices

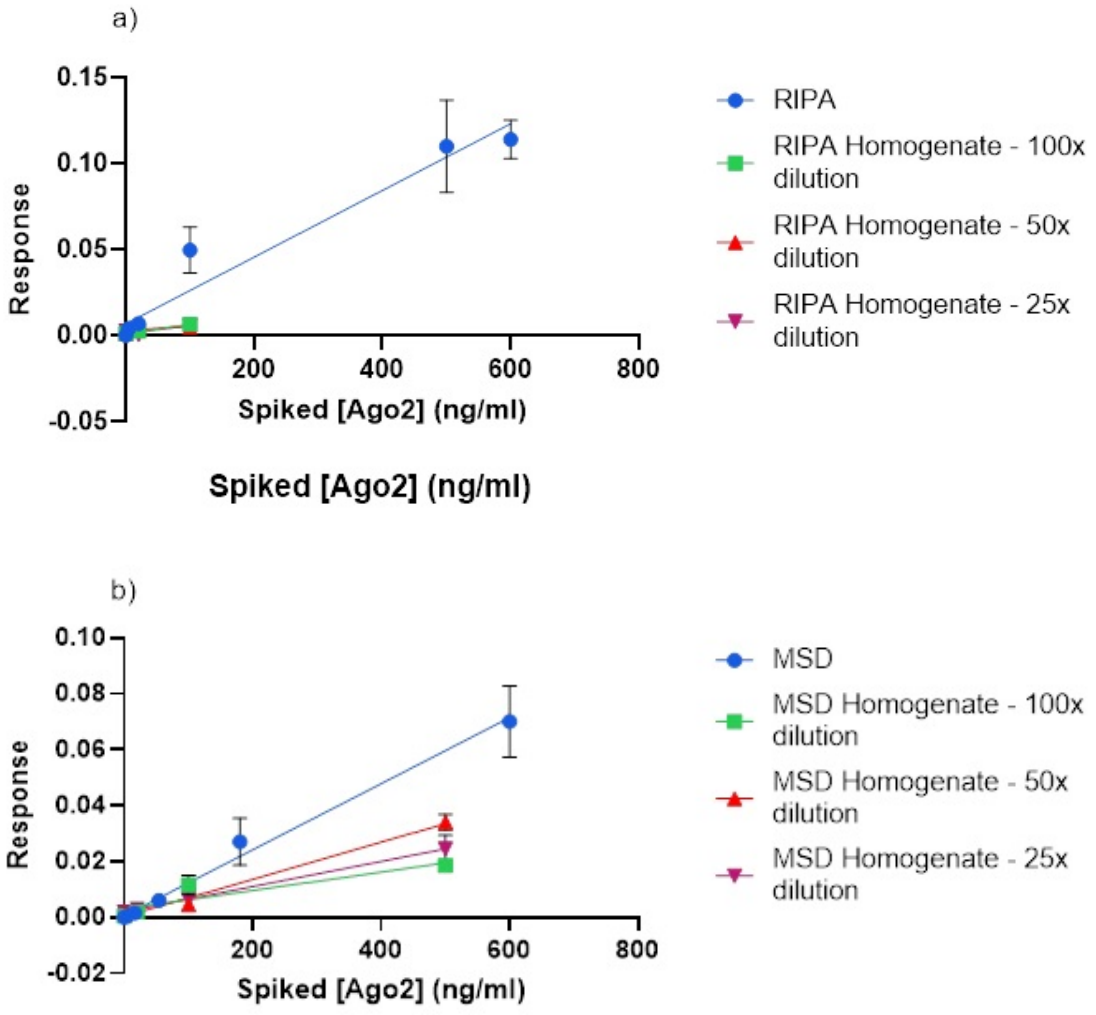


**Figure 3.15:** Average response with standard deviation vs the concentration of recombinant Ago2 that was spiked into samples containing either RIPA (a)) or MSD (b)) lysis buffers. Points at 2000 ng/ml of Ago2 are excluded from the plots.

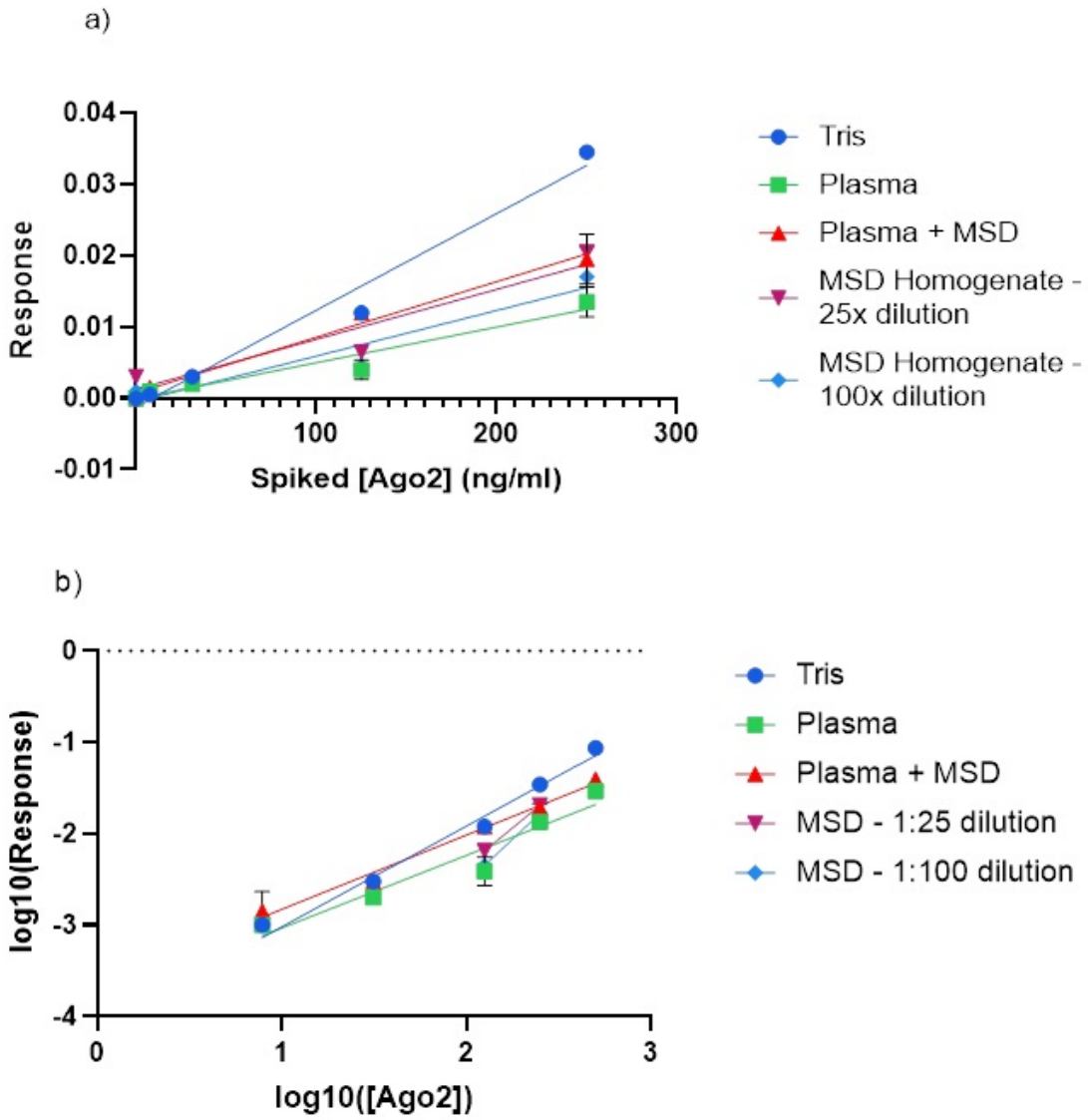


**Figure 3.16:** Average response with standard deviation vs the concentration of recombinant Ago2 after IP of curves in 50 mM tris, plasma diluted with tris, plasma diluted with MSD lysis buffer MSD homogenate diluted 25 or 100 times (a), as well as a log/log plot of the same (b). Note that the data points at 0 ng/ml of spiked in Ago2 have been excluded in b)

### 3.3.3 Extending the Extraction to Heart and Kidney

All work presented up until this point has focused on either buffer systems or homogenates of liver. To explore the applicability of the assay in other tissue it was applied to mouse heart and kidney tissue as well.
Performing IP in liver and heart tissue homogenised with RIPA or MSD lysis buffers revealed that the method could be used in either tissue (Figure 3.17). It also appeared that the amount of Ago2 in the kidney was lower than that in the heart.

Similarly, performing IP in liver and kidney showed that the amount of Ago2 in the kidney appeared to be lower than that in liver (Figure 3.18). Note that the data for liver has been displayed previously (Figure 3.12).

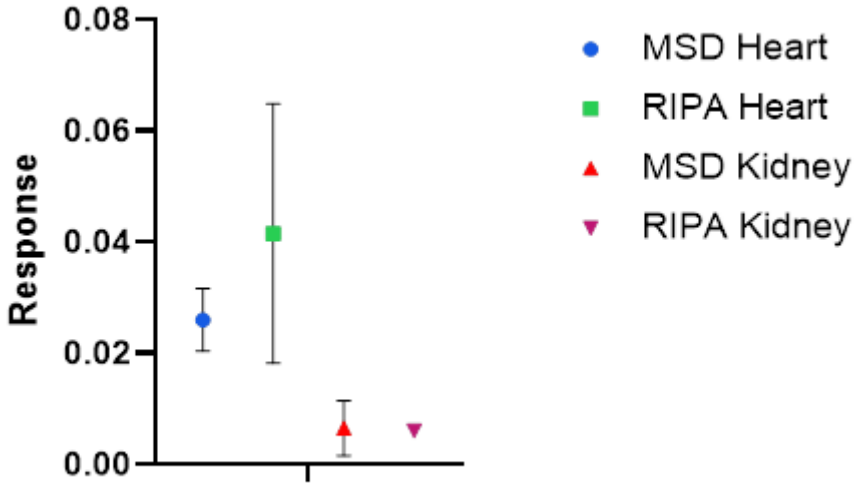


**Figure 3.17:** Mean response with standard deviations after IP in heart and kidney tissue homogenized with RIPA or MSD lysis buffers.

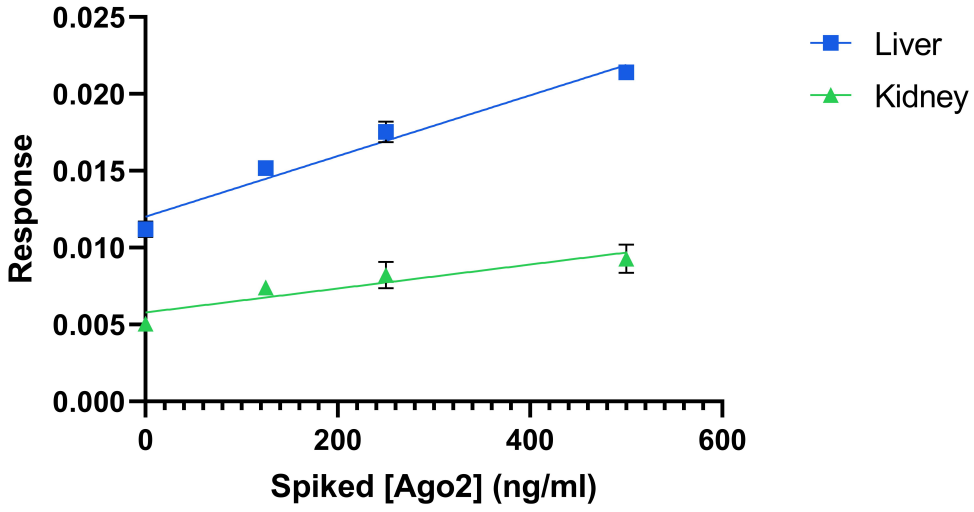


**Figure 3.18:** Mean response with standard deviations after IP in heart and kidney tissue homogenized with RIPA or MSD lysis buffers

## 3.4 RISC quantification *in vitro*

### 3.4.1 Evaluation of Sensitivity and the Impact of Non-Specific Binding

After exploring what parameters are best suited to maximise extraction of Ago2 the focus on to how to quantify the siRNA loaded into risk. In an example from the literature, siRNA was loaded into RISC in vitro by incubating siRNA in liver homogenate (Pei et al., 2010). As this would serve as a suitable test to whether RISC could be extracted whole and quantified using the method developed until this point. A tool compound siRNA, SOD1, was selected as the RNA to be incubated. In previous work a second siRNA, MALAT1, has been used as IS and as such it was selected serve in the same role in this project.

Two main issues were identified that could hinder the accurate quantification of the siRNA loaded into RISC. The potential for a loss of signal due to non-specific binding of the siRNA to the plate or tube a sample was stored in, and the sensitivity of the instrument to be used and. Based on previous work, it was determined that the non-specific binding could be reduced by diluting the samples with plasma crashed with methanol and diluted with deionized water. To test this and examine how low concentration of SOD1 that would be measurable, a standard curve was prepared via serial dilution of SOD1 according to the scheme in Table 3.4). Concentrations from 381.3 nM and below were analysed. The experiment was spread out over two days. On the first day, the curve was analysed in full in duplicate. On the second day the points at 0.5, 0.17 and 0.056 nM were analysed again. Only the antisense strand was measured in this experiment. The results (Figure 3.19) indicated that the instrument was sufficiently sensitive to detect SOD1 at concentrations at least as low as 0.056 nM, or 56 pM. As the response appeared to be consistent from day to day it also appeared that non-specific binding would not be an issue over the time span tested or that the diluted, crashed plasma had prevented any losses of SOD1.

| **Stock (uL)** | **Diluent (uL)** | **SOD1 (nM)** |
|---|---|---|
| 15 | | 151000 |
| 5 | 325 | 2287.9 |
| 50 | 250 | 381.3 |
| 50 | 100 | 127.1 |
| 50 | 100 | 42.4 |
| 50 | 100 | 14.1 |
| 50 | 100 | 4.7 |
| 50 | 100 | 1.6 |
| 50 | 100 | 0.5 |
| 50 | 100 | 0.17 |
| 50 | 100 | 0,056 |

**Table 3.4:** Dilution series of SOD1 siRNA to determine sensitivity of LCMS instrument to be use to quantify RISC loaded siRNA

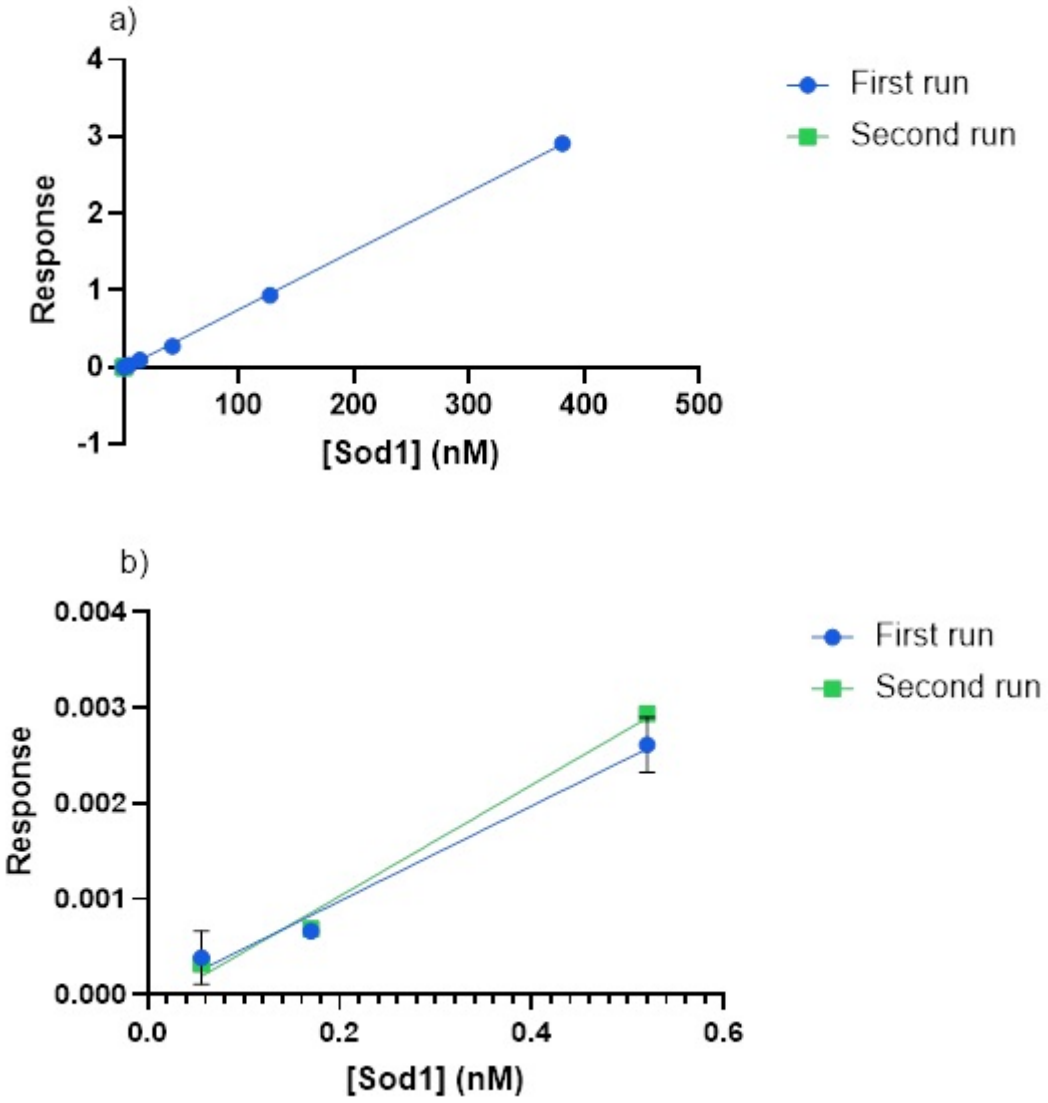


**Figure 3.19:** Mean response with standard deviations of antisense strand of SOD1, measured after analysis of standard curve prepared in crashed plasma that had been diluted with deionized water. Analysis was performed on two consecutive days. Responses for all concentrations are included in a) while only the points for the concentrations 0.5, 0.17 and 0.056 nM are included in b)

### 3.4.2 *In vitro* RISC Loading

Having established the sensitivity of the instrument and a solution to the problem of non-specific binding, an experiment was performed to attempt to replicate the in vitro loading of RISC. SOD1 siRNA duplex was incubated in homogenate containing MSD or RIPA lysis buffers at the concentrations 10, 2.5 and 5 µM at 37 °C overnight or for 4 hours. As a control and to ensure that not siRNA would be extracted without being complexed with RISC, the SOD1 duplex was also incubated with magnetic beads at a concentration of 10 µM. Analysis was then performed us-

ing two separate LCMS systems to quantify both SOD1 and Ago2.
The results from this experiment (Figure 3.20) were promising. The response of SOD1 appeared to be positively correlated with the concentration of that the homogenate contained. Also, it appeared that no extraction occurred when SOD1 was incubated with beads alone (Figure 3.21), indicating that extraction was due to the presence of antibody. This could be seen from the peaks corresponding to the MALAT1 IS being visible in both chromatograms while the peaks of transitions corresponding to SOD1 were visible only in a sample where antibodies were present during IP. This can be compared to the results for the quantification of Ago2 (Figure 3.20 b)). The response appeared to be consistent across the incubated concentration of SOD1, indicating that a similar amount of Ago2 was extracted in all samples. This further implied that eventual differences in amount of extracted siRNA would be due to the concentration of SOD1 in the homogenate, not due to variations in the extraction of Ago2.
As this experiment only quantified the antisense strand of SOD1 the possibility remained that RISC loading had not occurred properly and that the sense strand had not been degraded. To verify that only the antisense strand remained in the extracted complex the experiment was repeated. Again, SOD1 duplex was incubated for 4 hours at 37 °C in homogenate at the concentrations 5, 1.6 and 0.55 uM. As the highest response for both SOD1 and Ago2 were achieved in MSD homogenate, RIPA was excluded. To further investigate if the assay would be applicable to tissues beyond liver, homogenates of heart and kidney were also included.
As 2E1C-1C9 had previously been shown to be cross reactive with Ago proteins beyond Ago2 (Pei, 2010), a possible concern was that the loading of SOD1 into these other proteins might influence the quantification. To evaluate if this would influence the quantification of SOD1, antibody 2D4 was included in the experiment as well. By accident the slurry containing 2D4 was incubated with 9 ng antibody/µg bead, twice that of 2E1C-1C9. A standard curve was prepared by diluting SOD1 duplex in plasma crashed with methanol and diluted with deionized water as described in the Methods and Materials. The highest point in the standard curve, at 10 nM, was used to determine when the IS, the antisense strand and the sense strand would elute. By this method it appeared that the sense strand had been extracted by both 2D4 and 2E1C-1C9 (Figure 3.22)
Studying the extraction of Ago2 (Figure 3.23) revealed several interesting facts. Unlike in previous experiments, the highest extraction of Ago2 was achieved in heart rather than in liver. Notably the extraction appears to be highly consistent. The exception is in heart extracted with 2E1C-1C9 where the variability is high in all points.
The extraction in kidney was also very low for both antibodies while the extraction in liver was uncharacteristically low for 2E1C-1C9. The reasons for this are unclear. However, while it cannot be known for sure without repeating the experiment, as goes against many of the previous experiments it unlikely that the cause is due to some systematic issue with the immunoprecipitation itself.
Using the standard curve the amount of SOD1 sense and antisense strand that had been extracted were calculated (Figure 3.24). The highest amount of sense strand was measured in and kidney, with the levels in heart being very low in comparison.

This could be compared to the levels of the antisense strand where the opposite trend could be seen. Notably, the levels in heart were close to zero. Taken together this implied that SOD1 incubated in heart homogenate had correctly loaded into RISC, leading to the degradition of the passenger strand. It also appeared that this had occurred in a dose dependant manner. Consequently, it appeared that the same had not occurred in kidney and heart.
The results had implication for the applicability of the assay for all of the tested tissues. The fact that the extracted concentration of the sense strand were the highest in liver and kidney could indicate that RISC had not properly formed in those tissues, while very low concentrations of the sense strand in heart indicates that the assay could be applicable there The fact that 2D4 performed similarly to 2E1C-1C9 in this final experiment indicated that the risk of the other Ago proteins being extracted could be mitigated by using 2D4 instead.

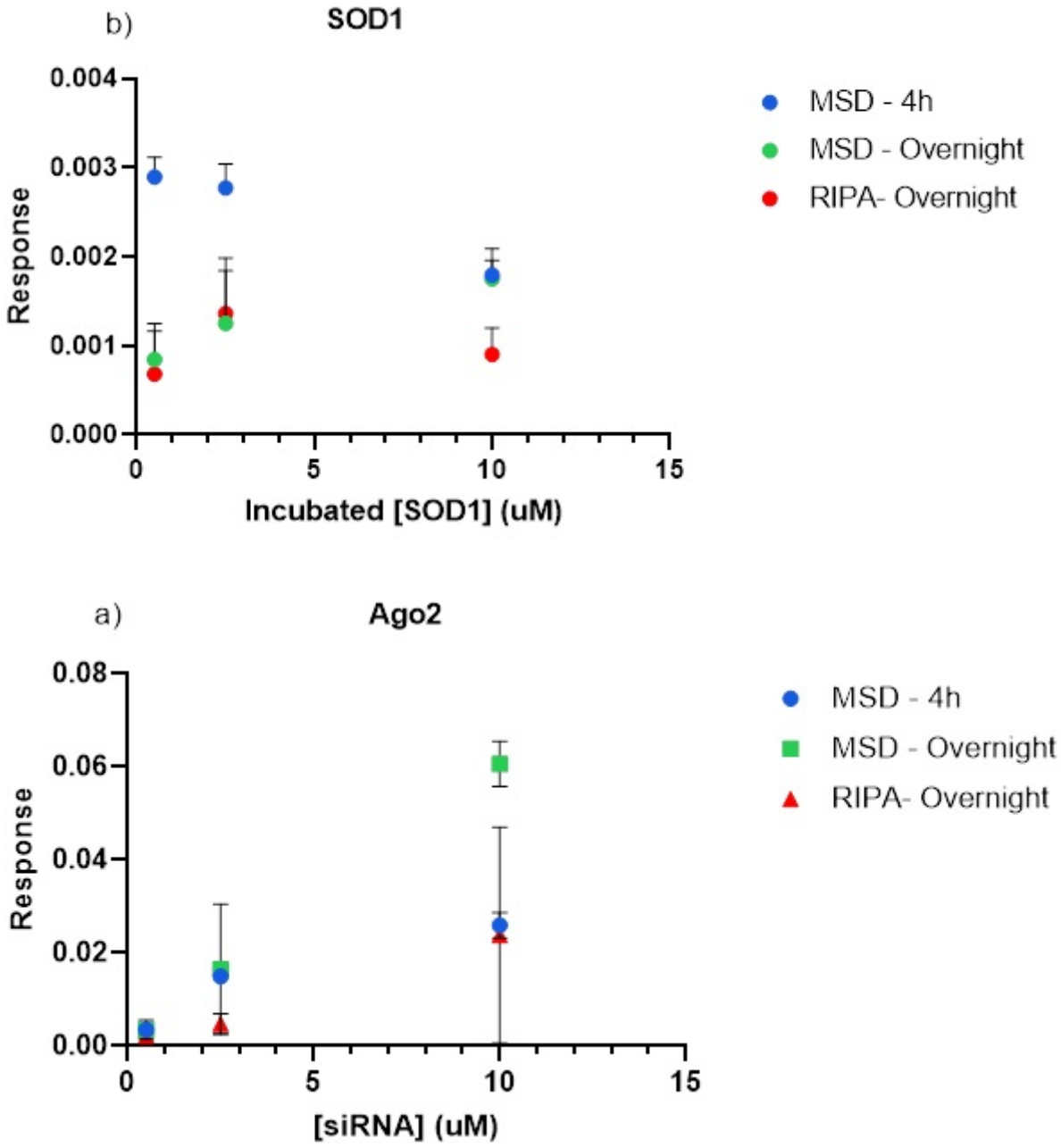


**Figure 3.20:** Mean response and standard deviation of response for SOD1 (a) and Ago2 (b) measured after incubation of 0.25, 5 and 10 uM of siRNA duplex in liver homogenates containing either MSD or RIPA lysis buffers.

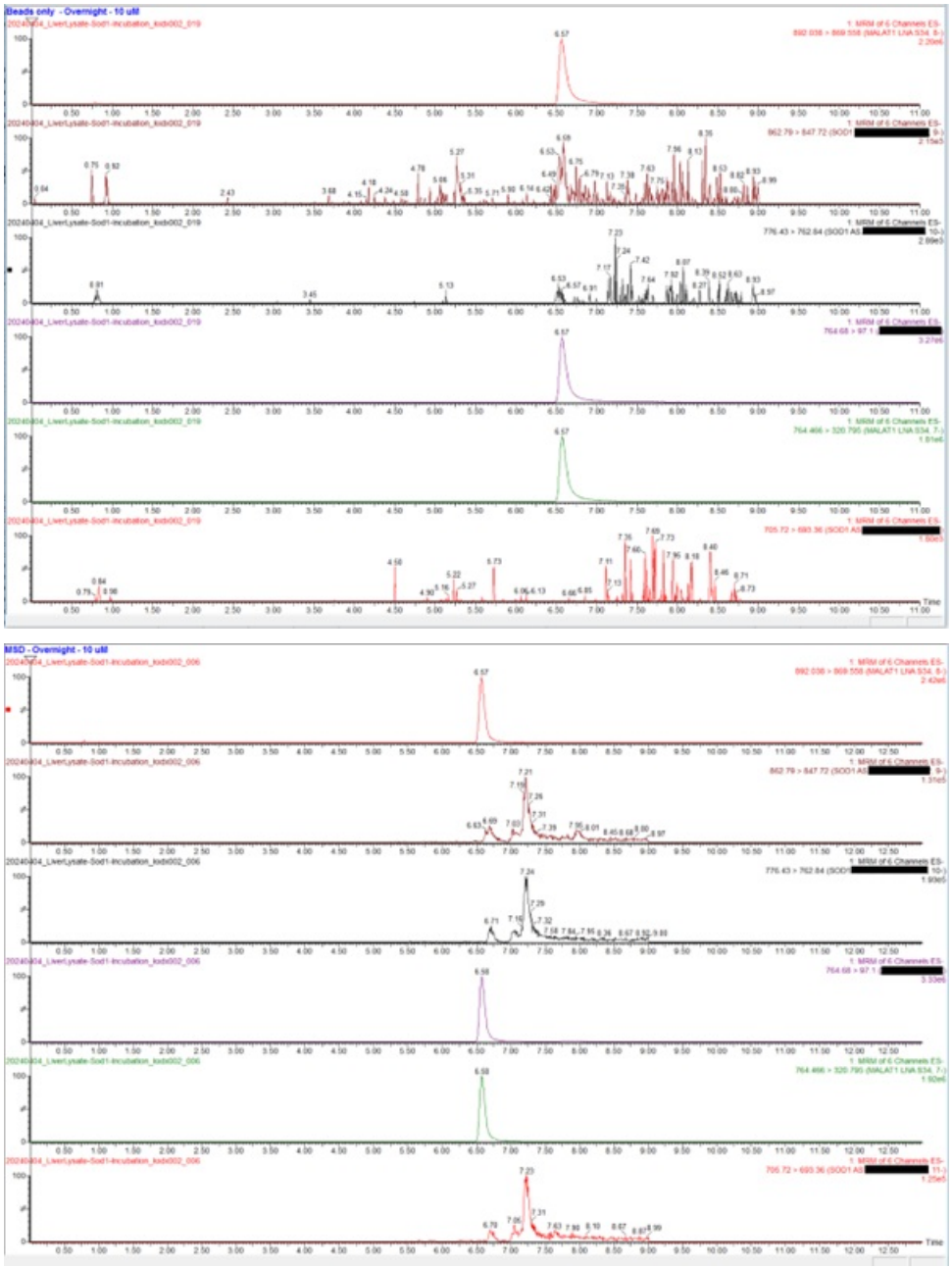


**Figure 3.21:** Chromatograms generated from samples where IP was performed with beads alone (top) or with beads conjugated to antibodies (bottom). Internal names of compounds have been blacked out. AS refers to the antisense strand.

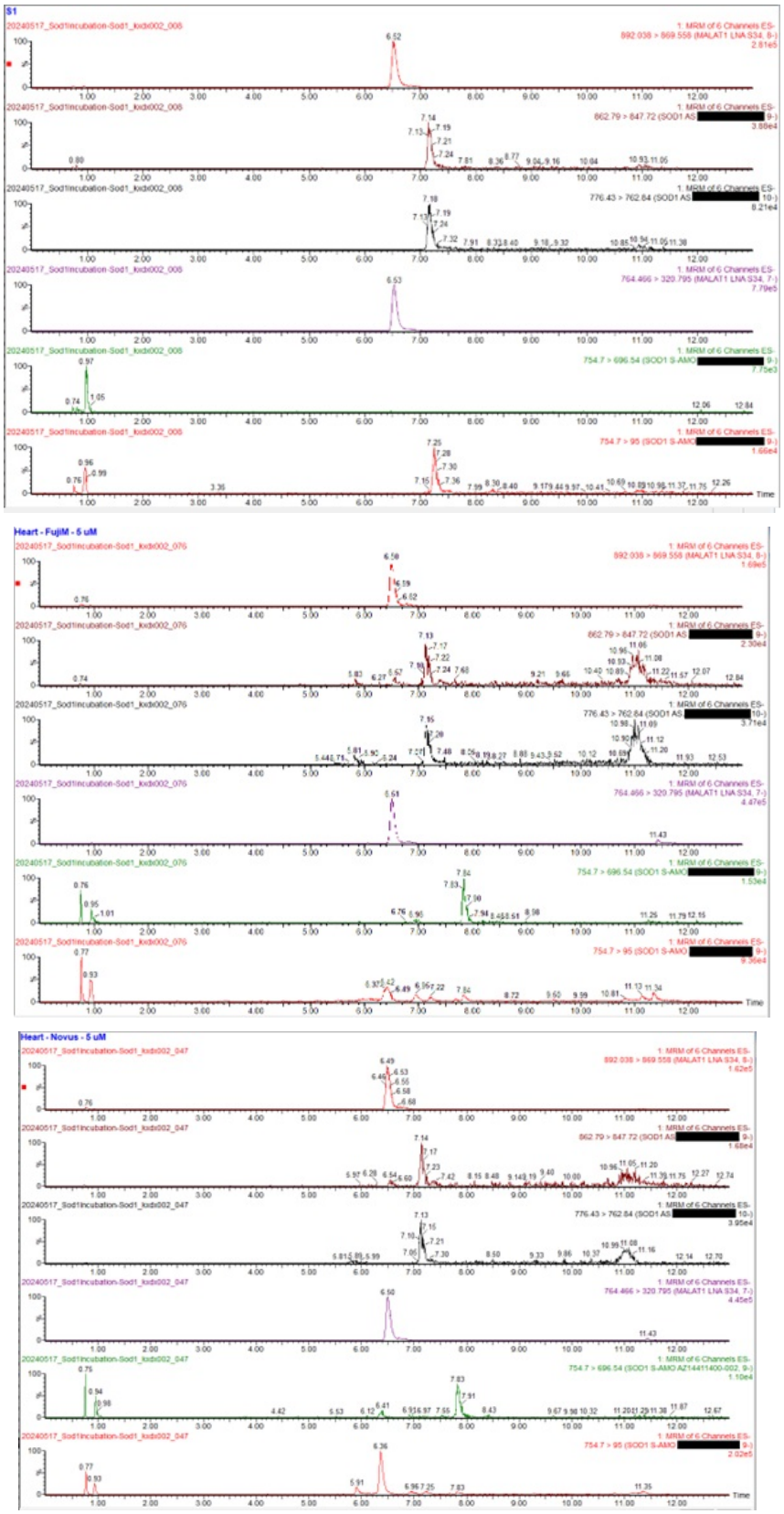

**Figure 3.22:** Chromatograms generated by analysis of duplex in standard curve (top) or heart homogenate incubated with 5 uM SOD1 duplex and subjected to IP using antibody 2D4 (middle) or 2E1C-1C9 (bottom).

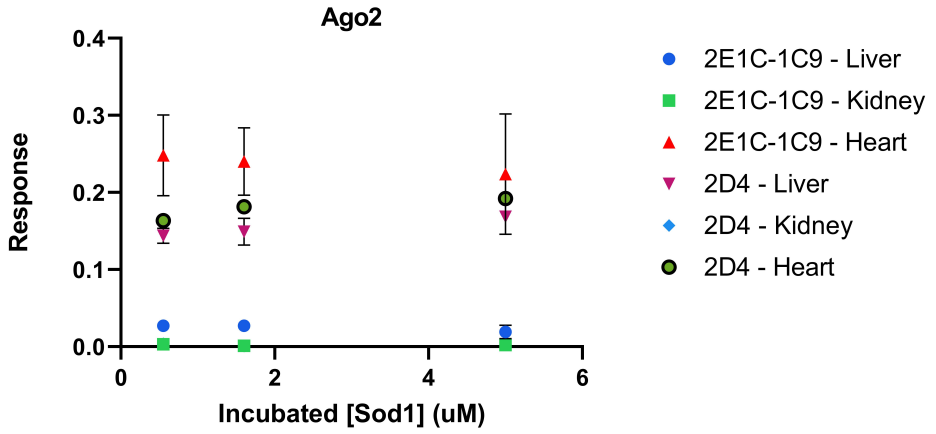


**Figure 3.23:** Mean response and standard deviation of Ago2 extracted from liver, kidney and heart homogenate with antibodies 2E1C-1C9 or 2D4

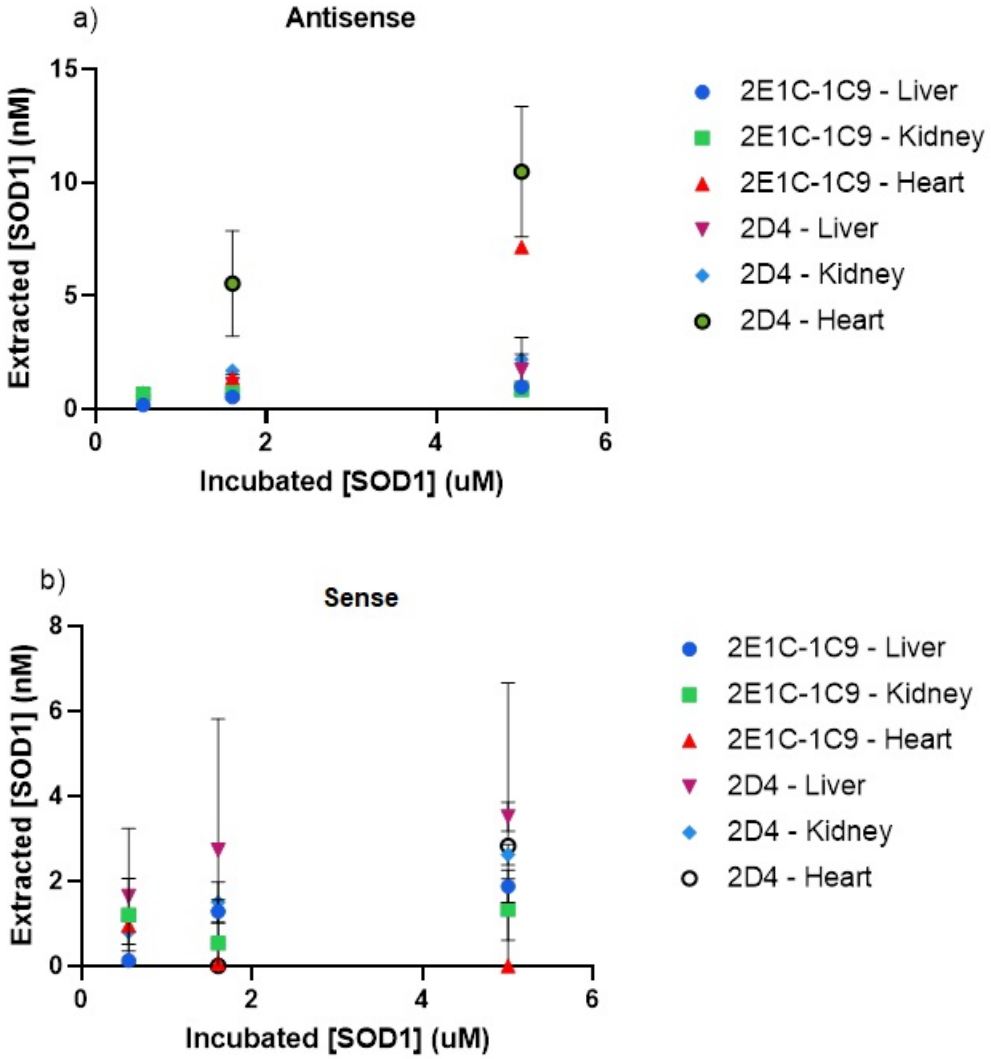


**Figure 3.24:** Calculated concentration of extracted siRNA and standard deviation of antisense (a) and sense strand (b) of SOD1 extracted from liver, kidney and heart homogenate with antibodies 2E1C-1C9 or 2D4. Data at 0.55 µM for 2D4-Heart is not included to a failure in the analysis.

# 4

# Conclusion and Future Perspective

At this point a method has been developed that can be used to evaluate RISC loading of specific siRNAs in vitro. The siRNA is incubated in homogenate to artificially induce RISC loading. The complex is then pulled out using immunoprecipitation with an anti-Ago2 antibody after which both Ago2 and the siRNA are quantified in parallel using LC-MS. It has been shown that RISC loading appears to occur correctly when SOD1 was incubated in heart, while the same could not be clearly shown in kidney and liver.

Previous publications have described methods to pull out RISC using immunoprecipitation and subsequently quantifying the amount of loaded siRNA (Flores-Jasso et al., 2012; Pei et al., 2010; Zheng et al., 2013). It is also not the first article how RISC can be formed in vitro and subsequently be quantified (Pei et al., 2010; Zheng et al., 2013). However, current published methods use qPCR as the method of quantification. As this technique is limited in being applicable solely to nucleotides it is unable to fully capture the dynamics of RISC since it is unable to account for changes in the level of Ago2. Also, while qPCR is highly sensitive and specific it requires the use of primers to quantify specific siRNA sequences (Arya et al., 2005). If, for example, the goal of a project is to screen a several siRNAs one would need to design and synthesise unique primers for each compound. This is both a slow and costly process making it an unattractive option if alternatives exist. By contrast, LC-MS is able to quickly and cheaply develop methods to quantify each compound that is to be screened, making it better suited for earlier stages of drug development. An additional advantage of LC-MS is the ability to quantify both Ago2 and the RISC loaded siRNA. By simultaneously measuring both components of RISC it would be possible to, for example, correct for differences in the RISC loading of a siRNA that are caused by changes in the intracellular level of Ago2.

Also, while previous publications have described methods to induce RISC loading in vitro they have done so by transfecting cell lines with siRNA (Zheng et al., 2013). The use of homogenised tissue is a potential advantage over this approach as the composition of the homogenate is presumably a closes match to that found in in vivo samples than in cell lines. While it has been suggested that the concentration of RISC loaded siRNA correlates better with gene knock down than the total intracellular concentration (Abrams et al., 2010), the results in this article have been correlated with in vivo data. To ensure that the assay is applicable to drug development this is a major step. The simplest way to do this would be to apply the assay to samples from animals that had been dosed with different siRNAs and then repeating the test by incubating the same siRNAs in blank homogenate. A possible issue with this approach is the sensitivity of LC-MS. Previous publications have

indicated that the amount of siRNA that is loaded into RISC at a given moment is very low, with perhaps only several hundred copies are loaded at a given time (Mesalchin et al., 2007; Pei et al., 2010; Veldhoen et al., 2006). This is presumably the main reason why qPCR is the main method used to quantify RISC loading as it has the necessary sensitivity to measure such low amounts.
The lack of a suitable surrogate matrix means that the assay can be used only for relative quantification of Ago2 at this point, and further studies are needed to find a matching surrogate or a conversion factor than can accurately be used to correct for this. While standard addition of recombinant protein to liver homogenate was shown to be a possible alternative, it requires larger amount of tissue to be homogenised than using a surrogate matrix . To avoid this, future research could further evaluate surrogate matrices. A all work of that nature in this article was performed using the antibody 2E1C-1C9. As 2D4 appeared to successfully extract Ago2 after the immunoprecipitation procedure had been optimised, it might be worthwhile to further evaluate the antibodies that were screened and discarded in this article work as they might not have the same issues as 2E1C-1C9.
A limitation with several of the results presented in this article is the high variability in the data points. While there might be several causes for this, it is observed in several of the data sets generated. One possible reason is the loss of beads during the immunoprecipitation. While any possible losses should always be mitigated, it could also be possible to compensate for them. By measuring the amount of beads that remains after all wash steps one could normalise the response of the analyte to this value and avoid the impact that losing beads would have. This could be done by, for example, including a transition for a surrogate peptide specific to the antibody used during IP or the streptavidin that the beads are coated with.
The assay described in this article should be a valuable tool in the study of siRNA therapeutics. As siRNAs must go through several steps before they can knock down their target genes. These steps being delivery, endosomal escape and RISC loading. The main strength of this assay is that it should allow researchers to gain a clearer picture of the entire chain of events and make better decisions on what aspects of the drug should be improved. The knock down of an siRNA in a tissue is lower than in another, this assay could be used to determine if RISC loading is the root cause. By being able to be applied in vitro, the assay should also be applicable in the early stages of drug development where several candidates are considered. If siRNAs that load poorly into RISC can be excluded early significant time and effort could be saved.

# References


Abrams, M., Koser, M. L., Seitzer, J., Williams, S., DiPietro, M. A., Wang, W., ... Sepp-Lorenzino, L. (2010). Evaluation of Efficacy, Biodistribution, and Inflammation for a Potent siRNA Nanoparticle: Effect of Dexamethasone Co-treatment. *Molecular Therapy*, *18*(1), 171–180. doi: 10.1038/mt.2009.208

Adams, D., Gonzalez-Duarte, A., O'Riordan, W. D., Yang, C.-C., Ueda, M., Kristen, A. V., ... Suhr, O. B. (2018). Patisiran, an RNAi Therapeutic, for Hereditary Transthyretin Amyloidosis. *New England Journal of Medicine*, *379*(1), 11–21. Retrieved from `https://www.nejm.org/doi/full/10.1056/NEJMoa1716153` doi: 10.1056/nejmoa1716153

Andersen, K. K., Oliveira, C. L., Larsen, K. L., Poulsen, F. M., Callisen, T. H., Westh, P., ... Otzen, D. (2009). The Role of Decorated SDS Micelles in Sub-CMC Protein Denaturation and Association. *Journal of Molecular Biology*, *391*(1), 207–226. Retrieved from `https://www.sciencedirect.com/science/article/pii/S0022283609007189` doi: 10.1016/j.jmb.2009.06.019

Arya, M., Shergill, I. S., Williamson, M., Gommersall, L., Arya, N., & Patel, H. R. H. (2005). Basic principles of real-time quantitative PCR. *Expert Review of Molecular Diagnostics*, *5*(2), 209–219. doi: 10.1586/14737159.5.2.209

Biscans, A., Coles, A., Haraszti, R., Echeverria, D., Hassler, M., Osborn, M., & Khvorova, A. (2018). Diverse lipid conjugates for functional extra-hepatic siRNA delivery in vivo. *Nucleic Acids Research*, *47*(3), 1082–1096. doi: 10.1093/nar/gky1239

Bults, P., Spanov, B., Olaleye, O., & Bischoff, R. (2019). Intact protein bioanalysis by liquid chromatography – High-resolution mass spectrometry. *Journal of Chromatography B*, *1110-1111*, 155–167. doi: 10.1016/j.jchromb.2019.01.032

Butler, J. S., Chan, A., Costelha, S., Fishman, S., Willoughby, J. L. S., Borland, T. D., ... Zimmermann, T. S. (2016). Preclinical evaluation of RNAi as a treatment for transthyretin-mediated amyloidosis. *Amyloid*, *23*(2), 109–118. doi: 10.3109/13506129.2016.1160882

Caplen, N. J., Parrish, S., Imani, F., Fire, A., & Morgan, R. A. (2001). Specific inhibition of gene expression by small double-stranded RNAs in invertebrate and vertebrate systems. *Proceedings of the National Academy of Sciences*, *98*(17), 9742–9747. doi: 10.1073/pnas.171251798

Cheng, W. L., Markus, C., Lim, C. Y., Tan, R. Z., Sethi, S. K., & Loh, T. P. (2022). Calibration Practices in Clinical Mass Spectrometry: Review and Recommendations. *Annals of Laboratory Medicine*, *43*(1), 5–18. Retrieved from `https://www.ncbi.nlm.nih.gov/pmc/articles/PMC9467832/` doi: 10.3343/alm.2023.43.1.5

Clark, K. D., Zhang, C., & Anderson, J. L. (2016). Sample Preparation for Bioanalytical and Pharmaceutical Analysis. *Analytical Chemistry*, *88*(23), 11262–11270. doi: 10.1021/acs.analchem.6b02935

Cristea, I. M., & Chait, B. T. (2011). Affinity Purification of Protein Complexes. *Cold Spring Harbor protocols*, *2011*(5), pdb.prot5611-pdb.prot5611. doi: 10.1101/pdb.prot5611

DeCaprio, J., & Kohl, T. O. (2020). Immunoprecipitation. *Cold Spring Harbor Protocols*, *2020*(11), pdb.top098509. doi: 10.1101/pdb.top098509

Dowdy, S. F. (2023). Endosomal escape of RNA therapeutics: How do we solve this rate-limiting problem? *RNA*, *29*(4), 396–401. doi: 10.1261/rna.079507.122

Ebhardt, H. A. (2013). Selected Reaction Monitoring Mass Spectrometry: A Methodology Overview. *Methods in molecular biology*, 209–222. doi: 10.1007/978-1-62703-631-3{_}16

Fire, A., Xu, S., Montgomery, M. K., Kostas, S. A., Driver, S. E., & Mello, C. C. (1998). Potent and specific genetic interference by double-stranded RNA in Caenorhabditis elegans. *Nature*, *391*(6669), 806–811. doi: 10.1038/35888

Flores-Jasso, C. F., Salomon, W. E., & Zamore, P. D. (2012). Rapid and specific purification of Argonaute-small RNA complexes from crude cell lysates. *RNA*, *19*(2), 271–279. doi: 10.1261/rna.036921.112

German, C. A., & Shapiro, M. D. (2019). Small Interfering RNA Therapeutic Inclisiran: A New Approach to Targeting PCSK9. *BioDrugs*, *34*(1), 1–9. doi: 10.1007/s40259-019-00399-6

Gilleron, J., Querbes, W., Zeigerer, A., Borodovsky, A., Marsico, G., Schubert, U., ... Zerial, M. (2013). Image-based analysis of lipid nanoparticle-mediated siRNA delivery, intracellular trafficking and endosomal escape. *Nature Biotechnology*, *31*(7), 638–646. Retrieved from `https://pubmed.ncbi.nlm.nih.gov/23792630/` doi: 10.1038/nbt.2612

Goyon, A., Yehl, P., & Zhang, K. (2020). Characterization of therapeutic oligonucleotides by liquid chromatography. *Journal of Pharmaceutical and Biomedical Analysis*, *182*, 113105. doi: 10.1016/j.jpba.2020.113105

Hammond, S. M., Aartsma-Rus, A., Alves, S., Borgos, S. E., Buijsen, R. A. M., Collin, R. W. J., ... Arechavala-Gomeza, V. (2021). Delivery of oligonucleotide-based therapeutics: challenges and opportunities. *EMBO Molecular Medicine*, *13*(4). Retrieved from `https://www.ncbi.nlm.nih.gov/pmc/articles/PMC8033518/pdf/EMMM-13-e13243.pdf` doi: 10.15252/emmm.202013243

Hendrickson, D. G., Hogan, D. J., Herschlag, D., Ferrell, J. E., & Brown, P. O. (2008). Systematic Identification of mRNAs Recruited to Argonaute 2 by Specific microRNAs and Corresponding Changes in Transcript Abundance. *PLoS ONE*, *3*(5), e2126. doi: 10.1371/journal.pone.0002126

Hu, B., Zhong, L., Weng, Y., Peng, L., Huang, Y., Zhao, Y., & Liang, X.-J. (2020). Therapeutic siRNA: state of the art. *Signal Transduction and Targeted Therapy*, *5*(1), 1–25. Retrieved from `https://www.nature.com/articles/s41392-020-0207-x` doi: 10.1038/s41392-020-0207-x

Iwakawa, H.-o., & Tomari, Y. (2022). Life of RISC: Formation, action, and degradation of RNA-induced silencing complex. *Molecular Cell*, *82*(1), 30–43. doi:

10.1016/j.molcel.2021.11.026

Jeanne Dit Fouque, D., Maroto, A., & Memboeuf, A. (2018). Internal Standard Quantification Using Tandem Mass Spectrometry of a Tryptic Peptide in the Presence of an Isobaric Interference. *Analytical Chemistry*, *90*(24), 14126–14130. doi: 10.1021/acs.analchem.8b05016

Kim, Y.-K. (2022). RNA therapy: rich history, various applications and unlimited future prospects. *Experimental & Molecular Medicine*, *54*(4), 455–465. Retrieved from `https://www.nature.com/articles/s12276-022-00757-5` doi: 10.1038/s12276-022-00757-5

Korfmacher, W. A. (2005). Foundation review: Principles and applications of LC-MS in new drug discovery. *Drug Discovery Today*, *10*(20), 1357–1367. doi: 10.1016/s1359-6446(05)03620-2

Kotapati, S., Deshpande, M., Jashnani, A., Thakkar, D., Xu, H., & Dollinger, G. (2021). The role of ligand-binding assay and LC–MS in the bioanalysis of complex protein and oligonucleotide therapeutics. *Bioanalysis*, *13*(11), 931–954. doi: 10.4155/bio-2021-0009

Li, J., Smith, L. S., & Zhu, H.-J. (2021). Data-independent acquisition (DIA): An emerging proteomics technology for analysis of drug-metabolizing enzymes and transporters. *Drug Discovery Today: Technologies*, *39*, 49–56. doi: 10.1016/j.ddtec.2021.06.006

Liu, A., Cheng, M., Zhou, Y., & Deng, P. (2022). Bioanalysis of Oligonucleotide by LC–MS: Effects of Ion Pairing Regents and Recent Advances in Ion-Pairing-Free Analytical Strategies. *International Journal of Molecular Sciences*, *23*(24), 15474. doi: 10.3390/ijms232415474

Liu, J. (2004). Argonaute2 Is the Catalytic Engine of Mammalian RNAi. *Science*, *305*(5689), 1437–1441. doi: 10.1126/science.1102513

Ma, H., Zhang, J., & Wu, H. (2014). Designing Ago2-specific siRNA/shRNA to Avoid Competition with Endogenous miRNAs. *Molecular Therapy - Nucleic Acids*, *3*, e176. doi: 10.1038/mtna.2014.27

MacLean, B., Tomazela, D. M., Abbatiello, S. E., Zhang, S., Whiteaker, J. R., Paulovich, A. G., ... MacCoss, M. J. (2010). Effect of Collision Energy Optimization on the Measurement of Peptides by Selected Reaction Monitoring (SRM) Mass Spectrometry. *Analytical Chemistry*, *82*(24), 10116–10124. doi: 10.1021/ac102179j

Mann, M., & Kelleher, N. L. (2008). Precision proteomics: The case for high resolution and high mass accuracy. *Proceedings of the National Academy of Sciences*, *105*(47), 18132–18138. doi: 10.1073/pnas.0800788105

Martindale, J., Gorospe, M., & Idda, M. (2020). Ribonucleoprotein Immunoprecipitation (RIP) Analysis. *BIO-PROTOCOL*, *10*(2). doi: 10.21769/bioprotoc.3488

Mescalchin, A., Detzer, A., Wecke, M., Overhoff, M., Wünsche, W., & Sczakiel, G. (2007). Cellular uptake and intracellular release are major obstacles to the therapeutic application of siRNA: novel options by phosphorothioate-stimulated delivery. *Expert opinion on biological therapy*, *7*(10), 1531–1538. doi: 10.1517/14712598.7.10.1531

Moosavi, S. M., & Ghassabian, S. (2018). Linearity of Calibration

Curves for Analytical Methods: A Review of Criteria for Assessment of Method Reliability. *Calibration and Validation of Analytical Methods - A Sampling of Current Approaches*. Retrieved from https://www.intechopen.com/books/calibration-and-validation-of-analytical-methods-a-sampling-of-current-approaches/linearity-of-calibration-curves-for-analytical-methods-a-review-of-criteria-for-assessment-of-method doi: 10.5772/intechopen.72932

Nair, J. K., Willoughby, J. L. S., Chan, A., Charisse, K., Alam, M. R., Wang, Q., ... Manoharan, M. (2014). Multivalent N-Acetylgalactosamine-Conjugated siRNA Localizes in Hepatocytes and Elicits Robust RNAi-Mediated Gene Silencing. *Journal of the American Chemical Society*, *136*(49), 16958–16961. doi: 10.1021/ja505986a

Nuckowski, , Kaczmarkiewicz, A., & Studzińska, S. (2018). Review on sample preparation methods for oligonucleotides analysis by liquid chromatography. *Journal of Chromatography B*, *1090*, 90–100. Retrieved from https://www.sciencedirect.com/science/article/pii/S1570023218302538?via%3Dihub doi: 10.1016/j.jchromb.2018.05.025

Pandey, S., Pandey, P., Tiwari, G., & Tiwari, R. (2010). Bioanalysis in drug discovery and development. *Pharmaceutical Methods*, *1*(1), 14. doi: 10.4103/2229-4708.72223

Panuwet, P., Hunter, R. E., D'Souza, P. E., Chen, X., Radford, S. A., Cohen, J. R., ... Barr, D. B. (2016). Biological Matrix Effects in Quantitative Tandem Mass Spectrometry-Based Analytical Methods: Advancing Biomonitoring. *Critical reviews in analytical chemistry / CRC*, *46*(2), 93–105. Retrieved from https://www.ncbi.nlm.nih.gov/pmc/articles/PMC4695332/#:~:text=In%20HPLC%20coupled%20with%20either doi: 10.1080/10408347.2014.980775

Paunovska, K., Loughrey, D., & Dahlman, J. E. (2022). Drug delivery systems for RNA therapeutics. *Nature Reviews Genetics*, *23*. doi: 10.1038/s41576-021-00439-4

Pei, Y., Hancock, P. J., Zhang, H., Bartz, R., Cherrin, C., Innocent, N., ... Barnett, S. F. (2010). Quantitative evaluation of siRNA delivery in vivo. *RNA*, *16*(12), 2553–2563. Retrieved from https://www.ncbi.nlm.nih.gov/pmc/articles/PMC2995415 doi: 10.1261/rna.2255810

Pino, L. K., Searle, B. C., Bollinger, J. G., Nunn, B., MacLean, B., & MacCoss, M. J. (2020). The Skyline ecosystem: Informatics for quantitative mass spectrometry proteomics. *Mass Spectrometry Reviews*, *39*(3), 229–244. Retrieved from https://www.ncbi.nlm.nih.gov/pmc/articles/PMC5799042/ doi: 10.1002/mas.21540

Pratt, A. J., & MacRae, I. J. (2009). The RNA-induced Silencing Complex: A Versatile Gene-silencing Machine. *Journal of Biological Chemistry*, *284*(27), 17897–17901. Retrieved from https://www.ncbi.nlm.nih.gov/pmc/articles/PMC2709356/ doi: 10.1074/jbc.r900012200

Roehr, B. (1998). Fomivirsen approved for CMV retinitis. *PubMed*, *4*(10), 14–16.

Seidler, J., Zinn, N., Boehm, M. E., & Lehmann, W. D. (2009).

**DEPARTMENT OF CHEMISTRY AND CHEMICAL ENGINEERING**
**CHALMERS UNIVERSITY OF TECHNOLOGY**
Gothenburg, Sweden
www.chalmers.se


CHALMERS
UNIVERSITY OF TECHNOLOGY